2017

Lignin modification to produce hydrophobic products

Alwadani, Norah

Lignin Modification to Produce Hydrophobic Products

by:
Norah Alwadani
Supervisor: Pedram Fatehi, PhD, P.Eng.

Thesis Presented to the Faculty of Graduate Studies
of Lakehead University of Thunder Bay
in Partial Fulfillment
of the Requirements
for the Degree of
Master of Science in Chemistry
Lakehead University
August 2017

Abstract

Kraft lignin is not widely utilized for industrial applications. In this MSc work, kraft lignin was modified by grafting hydrophobic groups to produce hydrophobic materials. The main objective was to study the grafting of lipophilic long alkyl chains on kraft lignin to improve its hydrophobicity. Dodecyl glycidyl ether was grafted at various molar ratios on kraft lignin in the presence of dimethyl benzyl amine catalyst. The influence of the grafting ratio of long alkyl chain to kraft lignin and methylated kraft lignin was comprehensively studied. The effect of grafting on the structure and thermal properties of lignin was investigated. The modified kraft lignin based products were characterised using a variety of methods including NMR, FTIR, TGA, DSC, GPC and elemental analysis, all of which demonstrated remarkable changes in the chemical and physical structure of kraft lignin after modification. The results showed that by increasing the grafting ratio, an increasing fraction of the phenolic hydroxy groups of lignin reacted with dodecyl glycidyl ether. Moreover, alterations in the surface tension of solvents and water containing modified kraft lignin as well as on the wettability of surfaces coated with modified kraft lignin were studied in detail.

Acknowledgements

First and foremost, I would like to thank Dr. Pedram Fatehi for his guidance and expertise during this research. I would also like to thank my committee members, Dr. B. Liao and Dr. S. Kinrade, for their advice throughout this project.

Additionally, I would like to thank the following group members Dr. Weijue Gao, Dr. Mohan Konduri, Dr. Yiqian Zhang and Dr. Jacquelyn Price, for helping me throughout my research. I would like to thank the past and present members of Dr. Fatehi's lab, for always keeping the time spent in the lab interesting. Last but not least, I wish to thank my husband, family, and friends for all of their love and support.

Dedication

To my parents and husband for all of their love, support, patience and encouragement.

Table of Contents

Title	Pages
Abstract	II
Acknowledgements	III
Table of Contents	V
List of Tables	VI
List of Figures	VII
List of Schemes	IX
Chapter	
1. Introduction	1
2. Literature Review	6
3. Experiments and methodology Analysis	23
4. Results and Discussions	39
5. Conclusion and Recommendations	79

List of Tables

Table 2.1: Compositions of different lignins. 9

Table 2.2: Inter-monolignolic linkages as percentages of total linkages in lignin. 10

Table 2.3: Properties of some industrial lignins (Oveissi and Fatehi, 2015; Vishtal and Kraslawski, 2011; Yang et al., 2015). 11

Table 2.4: Lignosulfonate properties. 13

Table 4.1: The hydroxyl content analysis of KL and MKL by an automatic potentiometric titrator and ^{31}P NMR. 45

Table 4.2: The properties of KL and MKL. 47

Table 4.3: Quantification of hydroxyl groups of KL before and after reaction with DGE using ^{31}P NMR. 51

Table 4.4: The characteristics of KL-DGE product. 52

Table 4.5: The characteristics of methylated kraft lignin based products. 55

Table 4.6: Properties of kraft lignin and lignosulfonate. 57

Table 4.7: Thermal degradation temperatures at 10% ($T_{10\%}$) and 50% ($T_{50\%}$) weight loss of lignin samples, and ash content of lignin samples left at 700 °C (R_{700}). 60

Table 4.8: Thermal properties of kraft lignin derivatives measured by DSC. 62

List of Figures

Figure 2.1: Structure of lignin macromolecule; p-hydroxyphenyl (green), guaiacyl (blue) and syringyl (red) units (after Zakzeski et al., 2010) 8

Figure 2.2: The representative structure of a lignosulfonate. 13

Figure 3.1: Overall reaction routes for producing DGE-grafted KL and DGE-grafted MKL. 24

Figure 3.2. Illustration of contact angles formed by sessile liquid droplet on a smooth solid surface. 32

Figure 4.1: ^{1}H NMR spectrum of the DGE in $CDCl_3$. 40

Figure 4.2: Quantitative ^{31}P NMR spectrum of kraft lignin (KL) and methylated kraft lignin (MKL) in pyridine/$CDCl_3$ mixture (1.6/1 v/v). 44

Figure 4.3: FT-IR spectrum of MKL and KL. 47

Figure 4.4: ^{31}P NMR spectrum of KL, KL-1, KL-2 and KL-3 in pyridine/$CDCl_3$ mixture (1.6/1 v/v). IS: internal standard. 50

Figure 4.5: FT-IR spectra of KL, KL-1, KL-2, and KL-3. 53

Figure 4.6: ^{31}P NMR spectra of MKL, MKL-1, MKL-2 and MKL-3 in pyridine/$CDCl_3$ mixture (1.6/1 v/v). IS: internal standard. 54

Figure 4.7: FT-IR spectra of MKL, MKL-1, MKL-2, and MKL-3. 56

Figure 4.8: a) Weight loss and b) weight loss rate of KL, KL-1, KL-2 and KL-3 conducted under N_2 at a flow rate of 30 mL/min with heating rate of 10 °C/min. 59

Figure 4.9: a) Weight loss and b) weight loss rate of MKL, MKl-1, MKL-2 and MKL-3 conducted under N_2 at a flow rate of 30 mL/min heated at 10 ℃/min. 60

Figure 4.10: The effect of concentration of KLs and MKLs on the contact angle of DMF. 64

Figure 4.11: Surface tension of DMF solutions containing KLs and MKLs at a concentration of 20 g/L and temperature of 22 °C. 65

Figure 4.12: Surface tension of DMF at various concentrations (200-1000 mg/L) of KLs or MKLs and room temperature. 66

Figure 4.13: Effect of a) KL derivatives and b) MKL derivatives interfacial tension between DMF and glass slide. 68

Figure 4.14: The effect of solvent on the contact angle of the surface coated with a) kraft lignin derivatives and b) methylated kraft lignin derivatives, recorded at 20 s and 22 ℃. 70

Figure 4.15: SEM images of glass slides coated with different solutions containing KL-3 10 g/L. 71

Figure 4.16: Contact angle of water droplet on a surface coated with kraft lignin derivatives at different spinning rates. 72

Figure 4.17: The effect of temperature of film formation on the contact angle of water droplet and coated glass slide (lignin derivatives in NH_4OH solution coated at 500 rpm). 73

Figure 4.18: Contact angle of water droplet on glass slide coated with KL, KL-3 and LS dissolved in ammonium hydroxide solution after 5 s and 20 s time intervals. 74

List of schemes

Scheme 4.1: The reaction route of epichlorohydrin and 1-dodecanol for glycidyl ether production. 39

Scheme 4.2: The reaction route for methylation of kraft lignin. 42

Scheme 4.3: Reaction of lignin and DGE in the presence of DMBA, where R= CH_2-$(CH_2)_{10}$-CH_3. 48

Chapter 1: Introduction

1.1 Overview

Currently, environmental, economical and supply issues are associated with the use of fossil fuel based products. Alternatively, chemicals with superior properties to fossil fuel ones can be produced from renewable resources (Hamaguchi et al., 2012; Jablonský et al., 2015). Currently, the production of different products from lignocellulosic biomass is being carried out throughout the world, especially in Canada (Ragauskas et al., 2006; Chen et al., 2014).

Lignocellulosic biomass consists primarily of cellulose, hemicelluloses, and lignin (Ragauskas et al., 2006; Oveissi and Fatehi, 2015). Lignin could be considered as a valuable resource for bio-based material production as it does not affect the food supply chain (in opposition to starch) and is considered an under-utilized by-product of the pulp and paper industry (Ragauskas et al., 2006; Chen et al., 2014).

As lignin could be converted to many value-added products via chemical modifications, it has been studied for a wide range of industrial applications such as composites, surfactants and dispersants (Alekhina et al., 2015; Norgren and Mackin, 2009; Rafati et al., 2012; Hazarika and Gogoi, 2014). Lignin is a complex polymer with hydrophobic rings and hydrophilic groups attached to the rings. Any chemical modification to lignin would alter its hydrophobic/hydrophilic nature, along with other properties, and thus its application (Wu et al., 2012; Konduri et al., 2015; Chen et al., 2014; Lin et al., 2014). Although numerous attempts at improving lignin's hydrophobicity using chemical modifications such as sulfonation, sulfomethylation, oxidation and phenolation have

been reported, the means by which lignin hydrophobicity may be enhanced still needs more investigation (Chen et al., 2014; Matsushita and Yasuda, 2005; Ouyang et al., 2009).

In this study, the effect of grafting dodecyl glycidyl ether on kraft lignin in the presence of dimethyl benzyl amine as a catalyst was investigated. The extent of grafting was controlled by use of methylation to mask the reactive phenolic hydroxyl groups on lignin. The primary objective of this work was to increase lignin's hydrophobicity by alkoxylation at different reactive sites and grafting ratios.

1.2 Objectives

The objectives of this thesis were to:

1. prepare lipophilic long chain dodecyl glycidyl ether to be utilized in kraft lignin modification;
2. modify kraft lignin via methylation;
3. improve the hydrophobicity of kraft lignin by grafting dodecyl glycidyl ether at different grafting ratios;
4. improve the hydrophobicity of methylated kraft lignin by grafting dodecyl glycidyl ether at various grafting ratios;
5. investigate the influence of grafting ratio of dodecyl glycidyl ether and methylation on the structure and thermal stability of lignin; and
6. investigate the impact of methylation and dodecyl glycidyl ether grafting on the surface tension, interfacial tension of N, N-dimethylformamide as well as wettability of glass slides coated with modified lignin.

Chapter one, which is the current chapter, covers the overall goals of this MSc thesis work. It also includes a brief summary of other chapters.

Chapter two reviews literature relevant to this work, which includes the properties, production, and extraction of lignin as well as reactions to enhance its hydrophilicity and/or hydrophobicity.

Chapter three discusses the materials and methods used in this thesis to characterize kraft lignin before and after modification.

Chapter four presents the results and discussion of this thesis.

Chapter five states the overall conclusions and future work of this thesis.

1.3. Novelty of this study

The study is novel as the following aspects have not been previously studied:

- The production of a novel lignin based product via methylation and alkoxylation with lipophilic long alkyl chains (dodecyl glycidyl ether).
- An investigation of the modified kraft lignin's properties, including its performance as hydrophobic material.

References

Alekhina, M., Ershova, O., Ebert, A., Heikkinen, S., Sixta, H. 2015. Softwood kraft lignin for value-added applications: Fractionation and structural characterization. Industrial Crops and Products, 66, 220-228.

Chen, C., Li, M., Wu, Y., Sun, R. 2014. Modification of lignin with dodecyl glycidyl ether and chlorosulfonic acid for preparation of anionic surfactant. RSC Advances, 4(33), 16944-16950.

Gharbi, R., Alajmi, A., Algharaib, M. 2012. The potential of a surfactant/polymer flood in a middle eastern reservoir. Energies, 5(12), 58-70.

Hamaguchi, M., Cardoso, M., Vakkilainen, E. 2012. Alternative technologies for biofuels production in kraft pulp mills-potential and prospects. Energies, 5(12), 2288-2309.

Hazarika, K., Gogoi, S. 2014. Comparative study of an enhanced oil recovery process with various chemicals for Naharkatiya oil field. International Journal of Applied Sciences and Biotechnology, 2(4), 432-436.

Jablonský, M., Botková, M., Kočiš, J. Šima, J. 2015. Characterization and comparison by UV spectroscopy of precipitated lignins and commercial lignosulfonates. In Cellulose chemistry and technology, 49(3-4), 267-274.

Konduri, M., Kong, F., Fatehi, P. 2015. Production of carboxymethylated lignin and its application as a dispersant. European Polymer Journal, 70, 371-383.

Lin, X., Zhou, M., Wang, S., Lou, H., Yang, D., Qiu, X. 2014. Synthesis, structure, and dispersion property of a novel lignin based polyoxyethylene ether from kraft lignin and poly(ethylene glycol). ACS Sustianable Chemistry and Engineering, 2, 1902-1909.

Matsushita, Y., Yasuda, S. 2005. Preparation and evaluation of lignosulfonates as a dispersant for gypsum paste from acid hydrolysis lignin. Bioresource Technology, 96, 465–470.

Norgren, M. Mackin, S. 2009. Sulfate and surfactants as boosters of kraft lignin precipitation. Industrial & Engineering Chemistry Research, 48(10), 5098-5104.

Ouyang, X., Ke, L., Qiu, X., Guo, Y., Pang, Y. 2009. Sulfonation of alkali lignin and its potential use in dispersant for cement. Journal of Dispersion Science and Technology, 30(1), 1-6.

Oveissi, F., Fatehi, P. 2015. Characterization of four different lignins as a first step toward the identification of suitable end-use applications. Journal of Applied Polymer Science, 132(32), 1-9.

Rafati, R., Hamidi, H., Idris, A., Manan, M. 2012. Application of sustainable foaming agents to control the mobility of carbon dioxide in enhanced oil recovery. Egyptian Journal of Petroleum, 21(2), 155-163.

Ragauskas, A., Williams, C., Davison, B., Britovsek, G., Cairney, J., Eckert, C., Frederick, W., Hallett, J., Leak, D., Liotta, C. 2006. The path forward for biofuels and biomaterials. Science, 311, 484–489.

Wu, H., Chen, F., Feng, Q., Yue, X. 2012. Oxidation and sulfomethylation of alkali extracted lignin from corn stalk. Bioresources, 7, 2742-2751.

Chapter 2: Literature Review

2.1. Introduction

The industrial production of a wide range of chemicals and synthetic polymers greatly relies on fossil based resources, which are becoming increasingly scarce and expensive. Therefore, pressure is growing on industries to practice sustainability and utilize renewable resources, which requires the development of environmentally sustainable feedstocks that are competitive in terms of cost, performance, availability, and logistical feasibility with the fossil-based materials they aim to replace. Moreover, global warming circumstances make it a necessity to replace the fossil-based products with biomass-based products (Hamaguchi et al., 2012; Jablonský et al., 2015). In this regard, lignocellulosic materials are considered as promising feedstocks, which are from plentiful, inexpensive and renewable resources (Elraies and Tan, 2012; Gharbi et al., 2012, Hamaguchi et al., 2012; Hazarika and Gogoi, 2014; Isikgor and Becer, 2015, Olajire, 2014).

Lignin is one of the main components of biomass, besides cellulose and hemicellulose, and is the second most abundant natural polymer after cellulose (El Mansouri et al., 2011; Hu et al., 2011; Tejado et al., 2007; Toledano et al., 2010; Watkins et al., 2015). Using lignin as a feedstock for producing value-added products has some advantages and disadvantages. In its favor, lignin is not used as food, but it is an under-utilized by-product of many food and pulping processes. Additionally, there are well-established commercial processes for producing different forms of lignin in a wide range of qualities and quantities. Increasing lignin use would also contribute to reduced greenhouse gas emissions. However, the downside is that lignin is a variable and chemically complex material which makes its utilization as a feedstock challenging (Jönsson et

al., 2008; Ragauskas et al., 2014; Satheesh Kumar et al., 2009). Although many products are commercially produced from cellulose, lignin has currently a limited commercial value. In the past, lignin has been mainly used as a fuel source, but recent studies have shown that it could be converted to many value-added products (Alekhina et al., 2015; Hazarika and Gogoi, 2014; Norgren and Mackin, 2009; Rafati et al., 2012). Lignin is a by-product of many chemical (e.g. kraft, sulfite, organosolv, soda, neutral sulfite semichemical (NSSC)) and biochemical (e.g. ethanol production) processes. Figure 2.1 depicts the complicated three-dimensional structure of a typical wood-derived lignin. It is clear that the chemical structure of lignin is complex, containing many functional groups such as carbonyl, benzyl alcohol, phenolic hydroxyl, and methoxyl, along with various types of linkages (Chen et al., 2014). The structure of lignin macromolecules can vary between plant species. It is also affected by wood treatment and the method of extraction (Toledano et al., 2010). As a result, the actual three-dimensional structure of lignin is often unknown without first engaging in detailed chemical investigations.

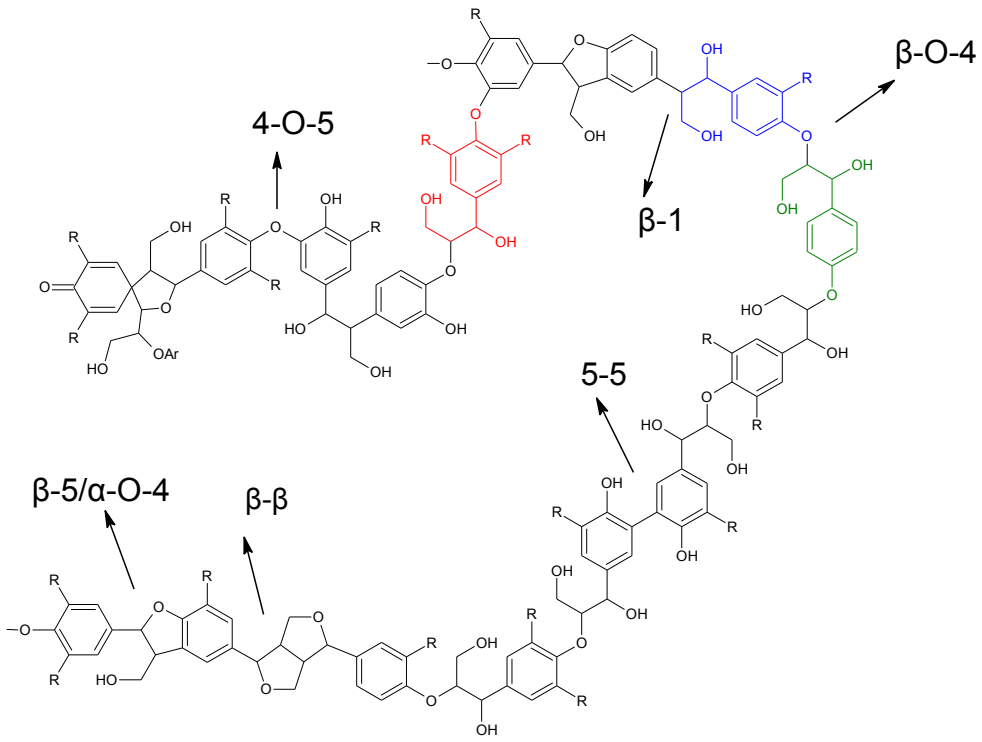

Figure 2.1: Structure of lignin macromolecule, revealing p-hydroxyphenyl (green), guaiacyl (blue) and syringyl (red) units (after Zakzeski et al., 2010).

Coniferyl (guaiacyl), sinapyl (synringyl), and *p*-coumaryl (*p*-hydroxyphenyl) alcohols are the main repeating units of lignin (Figure 2.1) (El Mansouri et al., 2011; Helander et al., 2013; Watkins et al., 2015). Table 2.1 lists lignin compositions obtained from different sources (Gosselink et al., 2010). It is evident that the number of hydroxyl groups, either aliphatic or aromatic, can differ depending on the lignin's origin. For instance, Indulin AT lignin (alkali lignin) has a higher number of hydroxyl groups compared to others, but it does not possess any syringyl units within its structure. In addition, hardwood soda and Lignosolv lignins may contain condensed structures, however, they likely contain lesser quantities of functional groups (aliphatic and aromatic hydroxyl groups) compared to other forms of lignin, which affects their chemical structure and application significantly.

Table 2.1: Compositions of different lignins

Lignin	Condensed structures (mmol/g)			Functional groups (mmol/g)		Reference
	Syringyl OH	Guaiacy OH	p-Hydroxyl OH	Aliphatic OH	Phenolic OH	
Indulin AT	NR	1.62	0.23	2.08	3.15	Gosselink et al., 2010
Sodium lignosulfonate	NR	NR	NR	1.07	2.01	Yang, et al., 2015
Curan 100	NR	1.84	NR	1.78	2.39	Gosselink et al., 2010
Switchgrass	NR	NR	NR	3.88	1.00	Sannigrahi et al., 2010.
Hardwood soda	0.92	0.51	0.34	1.34	2.48	Gosselink et al., 2010
Wheat Straw	NR	NR	NR	0.1	0.4–0.6	Lora and Glasser, 2002
Lignosolv hardwoods	1.05	0.7	0.2	1.08	2.71	Gosselink et al., 2010

NR: Not reported

Lignin of different origins (softwood or hardwood) possesses different percentages of the primary inter-unit linkages (Table 2.2 and Figure 2.1). For instance, biphenol bonds (5-5) in softwood lignin are three to five times more abundant than those in hardwood. Pinoresinol bonds (β-β) have the lowest abundance in both types of lignin. Phenyl coumarane, 1,2-diaryl propane, and biphenol (β-5, β-1, and 5-5, respectively) bonds make up 10% of the linkages in hardwood lignin, but are more abundant in softwood lignin. The 4-O-5 and α-O-4 bonds represent less than 10% of the total linkages, regardless of the wood source. Overall, the most abundant bonds in lignin are phenylpropane β−aryl ether (β-O-4) linkages, which are susceptible to pulping, bleaching and biological degradation reactions. Knowledge of which groups and linkages are present is important since they can behave very differently in terms of their reactivity with other chemicals (Brodin, 2009; Selyanina et al., 2007: Watkins et al., 2015).

Table 2.2: Inter-monolignolic linkages as percentages of total linkages in lignin

Types of linkage	Name	Linkages in lignin (%)	
		Softwood[1,2,4]	**Hardwood**[1,3,4]
β-O-4	Phenylpropane β−aryl ether	35-60	50-70
β-β	Pinoresinol	2-3	3-4
β-5	Phenyl coumarane	9-12	4-9
α-O-4	Phenylpropane α−aryl ether	6-8	7
β-1	1,2-Diaryl propane	7-10	7
5-5	Biphenol	18-25	≈5
4-O-5	Diaryl ether	4-8	7

1- Sannigrahi et al., 2010;
2- Santos et al., 2013;
3- Patil, 2012;
4- Brodin, 2009.

2.2. Lignin properties

The pulping industry remains the most significant lignin producer, with the sulfite and kraft processes being the two major techniques commercially used (Vishtal and Kraslawski, 2011). The lignin formed during the sulfite process is generally extracted as lignosulfonates, whereas that formed by the kraft method is usually burned as a fuel source. Lignosulfonates are of particular interest due to their high content of sulfonic acid functional groups attached to the aliphatic chain. This chemical composition renders them water soluble, with excellent binding and emulsifying properties. Kraft lignin, on the other hand, is much less soluble in water at neutral or acidic pH because of the lack of hydrophilic groups (Konduri et al., 2015; Qin et al., 2015; Vishtal and Kraslawski, 2011). Nevertheless, kraft lignin possesses several features distinguishing it from

other lignins. For instance, it contains a higher number of phenolic-OH compared to other types of lignin due to the extensive cleavage of β-aryl bonds during the pulping process.

Table 2.3 lists the properties of lignin extracted from spent kraft and sulfite pulping liquors. As can be seen, the properties (molecular weight, ash content, and polydispersity) vary according to the pulping process. The sulfite pulping process produces lignin with higher molecular weight (up to 150,000 g/mol) and ash content (up to 8 wt.%) than kraft lignin. Lignosulfonate also has a higher anionic charge density due to its high sulfonate group content.

Table 2.3: Chemical properties of some industrial lignins (Oveissi and Fatehi, 2015; Vishtal and Kraslawski, 2011; Yang et al., 2015).

Properties	**Kraft lignin**	**Lignosulfonate**
Molecular weight, Mw	1,500-5,000 (up to 25,000)	1,000-50,000 (up to 150,000)
Ash (wt.%)	0.5-3	4-8
Sugar (wt.%)	1-2.3	NR
Sulfur (wt.%)	1-3	3.5-8
Polydispersity (M_w/M_n)	2.5-3.5	4.2-7
Anionic charge density (meq/g)	0.76 ± 0.02	1.52 ± 0.02
Sulfonate group (meq/g)	NR	1.33 ± 0.2
Carboxylate groups (meq/g)	0.54 ± 0.03	0.11 ± 0.01
Hydrodynamic diameter (nm)	6.3 ± 0.7	10.1 ± 0.7

NR: Not reported

2.3. Lignin extraction process

Lignin is primarily extracted from spent pulping liquors, which also contain hemicellulose and inorganic impurities such as the pulping chemicals. Kraft lignin can easily be separated from black liquor by ultrafiltration and acidification (Qin et al., 2015; Vishtal and Kraslawski, 2011). The advantages of ultrafiltration are that it can be applied at any position in the mill (flexibility) and lignin can be separated without altering pH and temperature of the process. However, the extracted lignin needs further purification since it contains substantial amount of hemicellulose and ash, thereby increasing the overall cost of ultrafiltration (Qin et al., 2015; Vishtal and Kraslawski, 2011). LignoBoost and LignoForce are two acidification-based methods that have been recently developed to improve the ultrafiltration process. With LignoBoost, carbon dioxide is used to treat the black liquor to reduce its pH to 10, causing lignin to precipitate. The precipitates are dispersed, washed with acid, and then separated via filtration. This process has been found to increase the yield and purity of the produced kraft lignin, while simultaneously decreasing the operational costs by reducing the amount of sulfuric acid used and circumventing the need for use of larger filter as filter area can be kept small (Tomani P., 2010). The newest technology, LignoForce, uses a mixture of carbon dioxide and oxygen to concentrate, cool and precipitate spent liquor, which is then washed and pressed with filters. The resulting lignin has high purity, while carbon dioxide consumption is reduced as is the emission of hydrogen sulfide from acidification of black liquor.

2.4. Lignosulfonate application

Lignin recovered from spent sulfite pulping liquor has great potential as a surfactant (Jiao et al., 2007; Shulga et al., 2011), owing to the prevalence of hydrophilic sulfonate groups on the aliphatic side chains of hydrophobic aromatic rings (Elraies and Tan, 2012; Hong et al., 1987) as illustrated in Figure 2.2. Lignosulfonates are inexpensive and can be used as natural surfactants, dispersants and flocculants (Elraies and Tan, 2012; Tolosa et al., 2006).

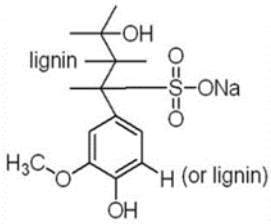

Figure 2.2: The representative structure of a lignosulfonate

Table 2.4 shows some chemical characteristics of lignosulfonates. It is observable that lignosulfonates have a significant amount of charge groups and varied molecular weight. The properties of lignosulfonate depend on their wood source as discussed earlier (Askvik et al., 1999; Ouyang et al., 2009; Vishtal and Kraslawski, 2011; Zhou et al., 2015).

Table 2.4: Lignosulfonate chemical characteristics

Parameters	**Zhou et al., 2015**	**Askvik et al., 1999**	**Vishtal and Kraslawski, 2011**	**Ouyang et al., 2009**
MW (g/mol)	13,021	62,700	1000-150,000	9,688
Surface charge (mmol/g)	1.73	NR	NR	NR
Polydispersity (M_w/M_n)	2.51	NR	4.2-7	3.02
Sulfonate groups (mmol/g)	1.33	6.2%	3.5-8%	NR
Carboxyl groups (mmol/g)	0.82	4.5%	NR	NR
Phenolic hydroxyl groups (mmol/g)	0.99	2.4%	NR	NR

NR: Not reported.

In addition to low production cost, the adsorption affinity, dispersability, and wettability of lignosulfonates (i.e. the tendency of a liquid to spread on a solid surface), they have been used in many applications. For example, they have been utilized as plasticizers in concrete, as emulsifiers and corrosion inhibitors in pesticides, and as ion-exchange resins (Borchardt, 1989; Calvo-Flores and Dobado, 2010; Elraies and Tan, 2012; Hong et al., 1987; Tejado et al., 2007). As also seen in

Table 2.4 lignosulfonates have excellent polydispersity properties. For instance, Grigg and Bai (2004) investigated the use of lignosulfonates as sacrificial agents for reducing the adsorption of other chemicals to porous materials for enhanced oil recovery application (Grigg and Bai, 2004).

On the other hand, lignosulfonates have a limited ability to decrease the interfacial tension of the oil−water interface or the surface tension of water (Perkins, 1998), which limits their applications. This is because lignosulfonates produced in the sulfite pulping process may be contaminated with polysaccharides and inorganic pulping chemicals (Hazarika and Gogoi, 2014).

Various schemes have been used to improve the charge density of lignosulfonates to widen their potential uses (Tolosa et al., 2006). For example, they have been used along with other synthetic and/or biological surfactants (either cationic or non-ionic) such as *n*-hexanol, *n*-heptanol, and alkyl benzene sulfonates (Sheng, 2015; Tolosa et al., 2006).

2.5. Modification of lignin

The properties (e.g. interfacial activity, reactivity) of lignosulfonates can be engineered by means of chemical modification. Similarly, other lignin sources, such as the kraft and soda lignin, can be modified for their potential uses in different applications (Dilling and Prazak, 1977; Hazarika and Gogoi, 2014; Jiao et al., 2007). Lignin can be subjected to many reactions such as alkylation, amination, carboxylation, acylation, halogenation, methylation, oxidation and reduction, sulfomethylation, sulfonation, and nitroxide formation that could modify its aromatic structure (Matsushita, 2015; Miller et al., 1999, 2002; Morrow, 1992; Pearl and Beyer, 1966). For example, hydrophilic functional groups can be introduced into the hydrophobic backbone by 1) substitution reactions introducing carboxylates, sulfates, or sulfonates to form anionic polymers, 2) reacting

with ammonium salts to form cationic polymers, or 3) reacting with alcohols (polyoxyethylenated chains) to form a more hydrophobic material.

2.6. Application of hydrophilic lignin derivatives

The chemical modifications of lignin result in different and improved properties. For example, introducing carboxylate groups into lignosulfonate molecules and using them under alkaline conditions increased their negative charges (Askvik, 2001). In another study, lignin was modified via alkylation, sulfonation, and oxidation to produce highly effective surfactants (Morrow, 1992). Moreover, a novel method was used to produce sulfonated benzyl alcohol/lignin phenol surfactant that is well suited to be used in the recovery of hydrocarbons from an oil field (Naae and Davis, 1992). He and Fatehi (2005) reported that softwood kraft lignin can be oxidized by nitric acid (20 wt% nitric acid at 100 °C for 1 h) and then sulfomethylated using formaldehyde and sodium metabisulfite (ratios of 1/1 and 0.5/1, respectively, at 100 °C for 3 h) to produce a water-soluble product with charge density of -3.87 meq/g which is effective at increasing the fluidity of cement admixtures. Ouyang et al. (2009) demonstrated that alkali lignin that is oxidized by hydrogen peroxide (30 wt% H_2O_2 for 1 h at 95 °C) and then sulfomethylated (37 wt% formaldehyde, sodium sulfite at 75 °C for 2 h) yields a product with lower surface tension in water than commercial lignosulfonate.

Another route for modifying lignin is the Mannich reaction (Laurichesse and Avérous, 2014). Yue et al. (2011), for example, carried out lignin amination in the presence of diethylamine and formaldehyde (at 75 °C and pH 11.5 for 3 h) to generate lignin-based products (as a glue) that showed a significant improvement in the performance of wood composites (Yue et al. 2011). In another work, a kraft lignin-based product was dissolved in NaOH solution and reacted with diethylenetriamine/formaldehyde (DETA/F) or N-(2-

aminoethyl)dehydroabietamide/diethylenetriamine/formaldehyde (DAEA/DETA/F) at 90 °C for 3 h (Liu et al., 2013). Whereas the kraft lignin reduced the surface tension of water to 45.62 mN/m, the modified lignin further reduced the surface tension of water to 29.85 mN/m at 5 g/L concentration (Liu et al., 2013).

2.7. Application of hydrophobic lignin derivatives

Many studies have reported different routes and ideas for lignin modification to change its hydrophobicity. It is claimed that hydrophobic lignin derivatives could have better interactions with other materials in organic solvents (Laurichesse and Avérous, 2014). The hydrophobicity of lignin can be improved via esterification and etherification, for example (Antonsson, 2007; Berlin and Balakshin, 2014; Laurichesse and Avérous, 2014). In one study, soda lignin was propylated via propylene oxide (37% concentration) under alkaline conditions for seven days at room temperature to produce propylated soda lignin (Ahvazi et al., 2011). This method generated a lignopolyol (propylated lignin) that had a potential use in polyurethane foams (Ahvazi et al., 2011). Furthermore, Gordobil and others (2016) have reported that esterification can improve the hydrophobicity of organosolv lignin (hardwood or softwood) to be used as a dispersant. In their study, organosolv lignins were dissolved in DMF and then reacted with dodecanoyl chloride at 20 °C for 2 h while using pyridine as a catalyst (Gordobil et al., 2016). The esterified lignin derivatives were found to be suited as a protective agent in wood products because of their high hydrophobicity and low glass transition temperature (Gordobil et al., 2016). Moreover, alkoxylation allows lignin derivatives to be used as components for production of polyurethane and polymer blends (Sen et al., 2015). The modified lignin may also have an application in paints and coatings, binders, flame retardants, water resistant composites, emulsifiers, and biomedicine (Sen et al., 2015). Hydrophobic lignin derivatives could also be used in unbleached pulp to improve its wet strength

and moisture adsorption (Antonsson, 2007). Others reported the use of lignin based hydrophobic products as antioxidants in plastics or compatibility mediator on strengthening pulp fibers in plastic composites (Antonsson, 2007). The improvement in hydrophobicity of lignin can be carried out via esterification with fatty acids or triglycerides and the product could be used in the production of polyesters, epoxy resins, and elastomeric materials (Ishikawa et al., 1961; Laurichesse and Avérous, 2014). In another work, soda lignin was esterified with maleic anhydride in 1,4-dioxane with 10/1 molar ratio to produce maleated lignins with high hydrophobicity characters to be used as polyols in polyurethane applications (Ahvazi et al., 2011). Further modification of this product as propylation (reaction with propylene oxide at room temperature for seven days) could improve the hydrophobicity of lignin even further (Laurichesse and Avérous, 2014). Moreover, Thielemans and others (Thielemans et al., 2001) reported that modified lignin with either maleic anhydride or epoxidize soybean oil could produce a product with potential use as a surface agent for fiber composites. Lignin would be suitable for biodegradable composites formation when it is combined with chitosan, which is a cationic polysaccharide. In this work, lignin was dissolved in 80 % aqueous acetic acid, and biodegradable blend films composed of chitosan, wherein lignin was successfully prepared via the solution-casting technique, which had a potential utilization in packaging (Chen et al., 2009).

Lignin may offer the potential to be a renewable, widely available, and inexpensive feedstock for different applications. Overall, the utilization of lignin and its modification to increase its industrial use is clearly worth considering as it does not compete with food (Laurichesse and Avérous, 2014). The properties of unmodified lignins make them inferior to existing commercial products in most applications. However, by chemically modifying lignin, improved properties can be engineered.

References

Ahvazi, B., Wojciechowicz, O., Ton-That, T., Hawari, J. 2011. Preparation of lignopolyols from wheat straw soda lignin. Journal of Agricultural and Food Chemistry, 59(19), 10505-10516.

Alekhina, M., Ershova, O., Ebert, A., Heikkinen, S., Sixta, H. 2015. Softwood kraft lignin for value-added applications: Fractionation and structural characterization. Industrial Crops and Products, 66, 220-228.

Antonsson, S. 2007. The use of lignin derivatives to improve selected paper properties. Royal Institute of Technology School of Chemical Science and Engineering Department of Fibre and Polymer Technology Division of Wood Chemistry and Pulp Technology. Doctoral thesis.

Askvik, K. 2001. Properties of the lignosulfonate–surfactant complex phase. Colloids and Surfaces A: Physicochemical and Engineering Aspects,182(1-3), 175-189.

Askvik, K., Are Gundersen, S., Sjöblom, J., Merta, J., Stenius, P. 1999. Complexation between lignosulfonates and cationic surfactants and its influence on emulsion and foam stability. Colloids and Surfaces A: Physicochemical and Engineering Aspects, 159(1), 89-101.

Berlin, A., Balakshin, M. 2014. Industrial lignins: Analysis, properties, and applications (Chapter 18). in: Bioenergy Research: Advances and Applications, Ed Gupta, V.G., Tuohy, M., Kubicek, CH.P., Saddler, J., Feng Xu, F. Elsevier, Amsterdam, 315-336.

Borchardt, J. 1989. Chemicals used in oil-field operations. ACS Symposium Series, 396, 3-54.

Brodin, I. 2009. Chemical properties and thermal behavior of kraft lignins. KTH Royal Institute of Technology. Stockholm University. Sweden. Licentiate Thesis.

Calvo-Flores, F., Dobado, J. 2010. Lignin as renewable raw material. ChemSusChem., 3(11), 1227-1235.

Chen, C., Li, M., Wu, Y., Sun, R. 2014. Modification of lignin with dodecyl glycidyl ether and chlorosulfonic acid for preparation of anionic surfactant. RSC Advances, 4(33), 16944-16950.

Chen, L., Tang, C., Ning, N., Wang, C., Fu, Q., Zhang, Q. 2009. Preparation and properties of chitosan/lignin composite films. Chinese Journal of Polymer Science, 27(05), 739-746.

Dilling, P. Prazak, G. 1977. Process for making sulfonated lignin surfactants. U.S. Patent. 4,001, 202.

El Mansouri, N., Yuan, Q., Huang, F. 2011. Characterization of alkaline lignins for use in phenol-formaldehyde and epoxy resins. Bioresource Technology, 6(3), 2647–2662.

Elraies, K., Tan, I. 2012. The Application of a new polymeric surfactant for chemical EOR, introduction to enhanced oil recovery (EOR) processes and bioremediation of oil-contaminated sites, Dr. Laura Romero-Zerón (Ed.), InTech, DOI: 10.5772/47975.

Gharbi, R., Alajmi, A., Algharaib, M. 2012. The potential of a surfactant/polymer flood in a middle eastern reservoir. Energies, 5(12), 58-70.

Gordobil, O., Herrera, R., Llano-Ponte, R., Labidi, J. 2016. Esterified organosolv lignin as hydrophobic agent for use on wood products. Progress In Organic Coatings, 103, 143-151.

Gosselink, R., van Dam, J., de Jong, E., Scott, E., Sanders, J., Li, J., Gellerstedt, G. 2010. Fractionation, analysis, and PCA modeling of properties of four technical lignins for prediction of their application potential in binders. Holzforschung, 64(2), 193-200.

Grigg, R., Bai, B. 2004. Calcium lignosulfonate adsorption and desorption on Berea sandstone. Journal of Colloid and Interface Science, 279(1), 36-45.

Hamaguchi, M., Cardoso, M., Vakkilainen, E. 2012. Alternative technologies for biofuels production in kraft pulp mills-potential and prospects. Energies, 5(12), 2288-2309.

Hazarika, K., Gogoi, S. 2014. Comparative study of an enhanced oil recovery process with various chemicals for Naharkatiya oil field. International Journal of Applied Sciences and Biotechnology, 2(4), 432-436.

He, W., Fatehi, P. 2015. Preparation of sulfomethylated softwood kraft lignin as a dispersant for cement admixture. The Royal Society of Chemistry/ Advance, 5(58), 47031-47039.

Helander, M., Theliander, H., Lawoko, M., Henriksson, G., Zhang, L., Lindström, M. 2013. Fractionation of technical lignin: molecular mass and pH effects. Bioresources, 8(2), 2270-2282.

Hong, S., Bae, J., Lewis, G. 1987. An evaluation of lignosulfonate as a sacrificial adsorbate in surfactant flooding. SPE Reservoir Engineering, 2(1), 17-27.

Hu, L., Pan, H., Zhou, Y., Zhang, M. 2011. Methods to improve lignin's reactivity as a phenol substitute and as replacement for other phenolic compounds: A brief review. BioResources, 6(3), 3515-3525.

Ishikawa, H., Oki, T., Fujita, F. 1961. Hydroxyethylation of phenolic hydroxyl groups in hard wood lignin. Mokuzai Gakkaishi (7), 85.

Isikgor, F., Becer, C. 2015. Lignocellulosic biomass: a sustainable platform for the production of bio-based chemicals and polymers. Polymer Chemistry, 6(25), 4497-4559.

Jablonský, M., Botková, M., Kočiš, J. Šima, J. 2014. Characterization and comparison by UV spectroscopy of precipitated lignins and commercial lignosulfonates. Cellulose Chemistry and Technology. 49(3-4), 267-274.

Jiao, Y., Xu, Z., Qiao, W., Li, Z. 2007. Research interfacial properties of the novel lignosulfonates. Energy sources, part A: Recovery, utilization, and environmental effects. 29(15), 1425-1432.

Jönsson, A., Nordin, A., Wallberg, O. 2008. Concentration and purification of lignin in hardwood kraft pulping liquor by ultrafiltration and nanofiltration. Chemical Engineering Research and Design, 86(11), 1271-1280.

Konduri, M., Kong, F., Fatehi, P. 2015. Production of carboxymethylated lignin and its application as a dispersant. European Polymer Journal, 70, 371-383.

Laurichesse, S., Avérous, L. 2014. Chemical modification of lignins: Towards biobased polymers. Progress in Polymer Science, 39(7), 1266-1290.

Liu, Z., Zhao, L., Cao, S., Wang, S., Li, P. 2013. Preparation and evaluation of a novel cationic amphiphilic lignin derivative with high surface activity. Bioresources, 8(4), 6111-6120.

Lora, J. Glasser, W. 2002. Recent industrial applications of lignin: A sustainable alternative to nonrenewable materials. Journal of Polymers and the Environment, 10(1-2), 39- 48.

Matsushita, Y. J. 2015. Conversion of technical lignins to functional materials with retained polymeric properties. Wood Science, 61(3), 230-250.

Miller, J. E., Evans, L. R., Mudd, J. E., Brown, K. A. 2002. Batch microreactor studies of lignin depolymerization by bases. 2. Aqueous Solvents. Albuquerque, New Mexico: Sandia National Laboratories, Report SAND2002-1318.

Miller, J. E., Evans, L., Littlewolf, A., Trudell, D. E. 1999. Batch microreactor studies of lignin and lignin model compound depolymerization by bases in alcohol solvents. Fuel., 78, 1363–1366.

Morrow, L. 1992. Enhanced oil recovery using alkylated, sulfonated, oxidized lignin surfactants. United States Patent 5,094,295.

Naae, D., Davis, C. 1992. Enhanced oil recovery using oil soluble sulfonates from lignin and benzyl alcohol. United States Patent 5,095,986.

Norgren, M., Mackin, S. 2009. Sulfate and surfactants as boosters of kraft lignin precipitation. Industrial & Engineering Chemistry Research, 48(10), 5098-5104.

Olajire, A. 2014. Review of ASP EOR (alkaline surfactant polymer enhanced oil recovery) technology in the petroleum industry: Prospects and challenges. Energy, 77, 963-982.

Ouyang, X., Ke, L., Qiu, X., Guo, Y., Pang, Y. 2009. Sulfonation of alkali lignin and its potential use in dispersant for cement. Journal of Dispersion Science and Technology, 30(1), 1-6.

Oveissi, F., Fatehi, P. 2015. Characterization of four different lignins as a first step toward the identification of suitable end-use applications. Journal of Applied Polymer Science, 132(32), 1-9.

Patil, R. 2012. Cleavage of acetyl groups for acetic acid production in kraft pulp mills. Chemical Engineering. University of Maine. Master Thesis.

Pearl, I., Beyer, D. 1966. Oxidation of alkali lignin. Advances in Chemistry, 59, 145-156.

Perkins, W.S. 1998. Surfactants: A primer. An in-depth discussion of the behavior of common types of surfactants. Dyeing, Printing and Finishing, ATI-Atlanta, USA., pp: 51-54.

Qin, Y., Yang, D., Guo, W., Qiu, X. 2015. Investigation of grafted sulfonated alkali lignin polymer as dispersant in coal-water slurry. Journal of Industrial and Engineering Chemistry, 27, 192-200.

Rafati, R., Hamidi, H., Idris, A., Manan, M. 2012. Application of sustainable foaming agents to control the mobility of carbon dioxide in enhanced oil recovery. Egyptian Journal of Petroleum, 21(2), 155-163.

Ragauskas, A., Beckham, G., Biddy, M., Chandra, R., Chen, F., Davis, M., Davison, B., Dixon, R., Gilna, P., Keller, M., Langan, P., Naskar, A., Saddler, J., Tschaplinski, T., Tuskan, G., Wyman, C. 2014. Lignin valorization: improving lignin processing in the biorefinery. Science, 344(6185), 1246843-1246843.

Salager, J. L. 2005. Surfactants types and uses. Firp Booklet, (E300-A).

Sannigrahi, P., Pu, Y., Ragauskas, A. 2010. Cellulosic biorefineries-unleashing lignin opportunities. Current Opinion in Environmental Sustainability, 2(5), 383–393.

Santos, R., Hart, P., Jameel, H., Chang, H. 2013. Wood based lignin reactions important to the biorefinery and pulp and paper industries. Bioresources, 8(1), 1456-1477.

Satheesh Kumar, M. N., Mohanty, A. K., Erickson, L., Misra, M. 2009. Lignin and its applications with polymers. Journal of Biobased Materials and Bioenergy, 3(1), 1-24.

Selyanina, S., Trufanova, M., Afanas'ev, N., Selivanova, N. 2007. Surfactant properties of kraft lignins. Russian Journal of Applied Chemistry, 80(11), 1832-1835.

Sen, S., Patil, S., Argyropoulos, D. 2015. Thermal properties of lignin in copolymers, blends, and composites: a review. Green Chemistry, 17(11), 4862-4887.

Sheng, J. 2015. Status of surfactant EOR technology. Petroleum, 1(2), 97-105.

Shulga, G., Shakels, V., Skudra, S., Bogdanovs, V. 2002. Modified lignin as an environmentally friendly surfactant. Environment Technology Resources. Proceedings of The International Scientific and Practical Conference. Tomsk, Russia. 1, 276-181.

Tejado, A., Peña, C., Labidi, J., Echeverria, J., Mondragon, I. 2007. Physico-chemical characterization of lignins from different sources for use in phenol–formaldehyde resin synthesis. Bioresource Technology, 98(8), 1655-1663.

Thielemans, W., Can, E., Morye, S., Wool, R. 2001. Novel applications of lignin in composite materials. Journal of Applied Polymer Science, 83(2), 323-331.

Toledano, A., García, A., Mondragon, I., Labidi, J. 2010. Lignin separation and fractionation by ultrafiltration. Separation and Purification Technology, 71(1), 38-43.

Tolosa, L., Rodríguez-Malaver, A., González, A., Rojas, O. 2006. Effect of Fenton's reagent on O/W emulsions stabilized by black liquor. Journal of Colloid and Interface Science, 294(1), 182-186.

Tomani, P. E. R. 2010. The lignoboost process. Cellulose Chemistry & Technology, 44(1), 53-58.

Vishtal, A., Kraslawski, A. 2011. Challenges in industrial applications of technical lignins. BioResources, 6(3), 3547-3568.

Watkins, D., Nuruddin, M., Hosur, M., Tcherbi-Narteh, A., Jeelani, S. 2015. Extraction and characterization of lignin from different biomass resources. Journal of Materials Research and Technology, 4(1), 26-32.

Yang, D., Li, H., Qin, Y., Zhong, R., Bai, M., Qiu, X. 2015. Structure and properties of sodium lignosulfonate with different molecular weight used as dye dispersant. Journal of Dispersion Science and Technology, 36(4), 532-539.

Yue, X., Chen, F., Zhou, X. 2011. Improved interfacial bonding of PVC/wood-flour composites by lignin amine modification. BioResources, 6(2), 2022-2044.

Zakzeski, J., Bruijnincx, P., Jongerius, A., Weckhuysen, B. 2010. The catalytic valorization of lignin for the production of renewable chemicals. Chemical reviews, 110(6), 3552-3599.

Zhou, M., Wang, W., Yang, D., Qiu, X. 2015. Preparation of a new lignin-based anionic/cationic surfactant and its solution behaviour. RSC Adv., 5(4), 2441-2448.

Chapter 3: Experiments and Analysis

3.1. Raw materials

Softwood kraft lignin (KL) was supplied by FPInnovations from its pilot plant facilities located in Thunder Bay, ON. Canada. 1-dodecanol (98%), epichlorohydrin (ECH), tetrabutyl ammonium bromide (TBAB), sodium hydroxide (98%), toluene, N,N-dimethylbenzylamine (BDMA), petroleum ether, hydrochloric acid (37%), dimethyl sulfoxide (DMSO), dimethyl sulfate, pyridine, deuterated chloroform ($CDCl_3$, 99.8%), cyclohexanol, chromium (III) acetylacetoate, 2-chloro-4,4,5,5-tetramethyl-1,2,3-dioxaphospholane (TMDP, 95%), N,N-dimethylformamide (DMF, 99.8%), poly(diallyldimethylammonium chloride) solution (PDADMAC; 100,000-200,000 g/mol, 20 wt.% in water), anionic polyvinyl sulfate (PVSK; 100,000-200,000 g/mol, 98.4 wt% esterified), potassium hydroxide solution (8 M), para-hydroxybenzoic acid, ammonium hydroxide (NH_4OH), methanol and phenolphthalein, all analytical grade, were purchased from Sigma Aldrich and used as received. Dialysis membrane with a molecular weight cut-off of 1000 g/mol was obtained from Spectrum Labs Inc., USA.

3.2. Reaction procedure

Figure 3.1 shows the reaction procedures followed to produce various modified lignins: 1) etherfying agent (dodecyl glycidyl ether, DGE) was prepared; 2) methylated kraft lignin (MKL) was also prepared via a methylation reaction and 3) DGE was grafted on KLMKL.

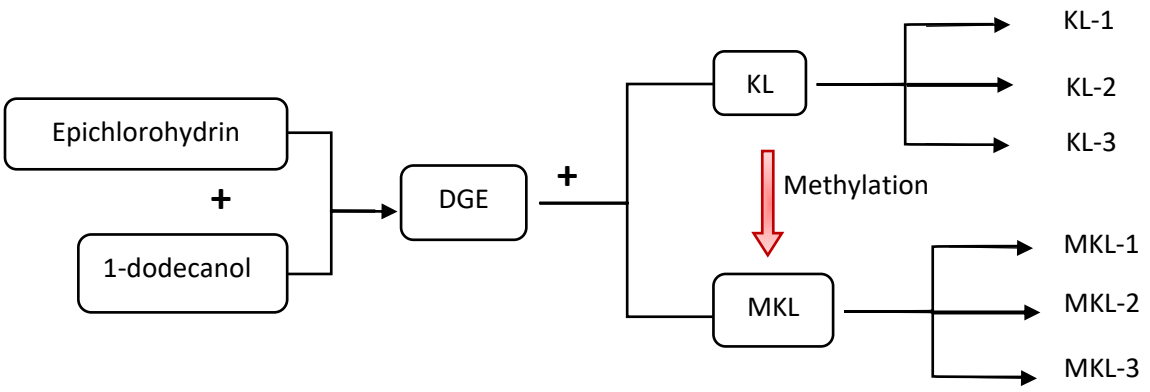

Figure 3.1: Overall reaction routes for producing DGE-grafted KL and DGE-grafted MKL.

3.3. Dodecyl glycidyl ether (DGE) preparation

The DGE was prepared according to the method described by Chen et al. (2014). 1-dodecanol was dissolved in toluene (0.99 mol) and combined with 25 g of 48 wt.% NaOH(aq) and 1.6 g of TBAB in a 250-mL round-bottom flask. 18.5 g of ECH were added dropwise at room temperature and stirring at 300 rpm, followed by heating at 50 °C for 6 h. The mixture was then quickly cooled by immersing the flask in water, whereupon it separated into an organic layer (the product in toluene) and an aqueous layer (unreacted materials). The organic layer was separated and purified by repeated washing with distilled water at 60 °C in a separatory funnel to extract unreacted materials. Then, the solvent was completely removed from the organic layer using a rotary evaporator **(**Rotaryevap Buchi R210) at room temperature under vacuum to obtain DGE. The product was chemically characterized.

3.4. Methylation of kraft lignin

To investigate the reaction of lignin with DGE, KL was methylated according to the procedure explained in the past (Sadeghifar et al., 2012; Kong et al., 2015; Argyropoulos et al., 2014; Sen et al., 2013). In this experiment, 1 g of KL was solubilized at room temperature in 15 mL of 0.7 M

NaOH via stirring at 300 rpm. Dimethyl sulfate was added to the mixture at a 1/2.5 molar ratio of phenolic hydroxyl group of lignin to dimethyl sulfate. At ambient temperature, the mixture was stirred for 30 min and then it was heated to 80 °C to react for 2 h. Due to the rapid hydrolysis of dimethyl sulfate producing sulfuric acid at the high ratio of methylation in this reaction, the pH dropped. Therefore, the pH of the mixture was maintained at 11 by continuously adding 0.7 M NaOH to the mixture throughout the experiment. After the reaction, the mixture was cooled to room temperature, and then the product (methylated kraft lignin, MKL) was precipitated by decreasing the pH to 2 by adding 2 M HCl. Afterward, the MKL was collected by filtration and thoroughly washed with deionized water until the sample pH reached neutrality. The MKL samples were then freeze dried under vaccum (Labconco, FreeZone 1L).

3.5. Lignin modification with dodecyl glycidyl ether (DGE)

KL and MKL were modified with DGE as described in the literature (Chen et al., 2014; Sadeghifar et al., 2012). In a 250-mL round-bottom three-neck glass flask equipped with a mechanical stirrer, 2 g of lignin was dissolved under vigorous stirring (400 rpm) in 80 mL DMSO. BDMA (0.45 g) was then added as a catalyst, followed by DGE at different molar ratios of lignin hydroxide functionality to DGE. Afterward, the mixture was purged with nitrogen gas to remove oxygen. The first 30 min of the reaction occurred at room temperature, and then the mixture was heated to 100 °C and reacted for another 5 h. The reaction was stopped by adding 2 M HCl (5 mL) and the mixture was stirred for another 30 min at room temperature to cool down. Petroleum ether was then added to facilitate the separation of different components via centrifugation at 1500 rpm for 5 minutes. The solvent (DMSO) was then removed from the mixture by dialysis while changing water every hour for the first six hours, every 6 h for a day, and finally twice more over the following day. The resulting water-insoluble product was separated via centrifugation at 1500 rpm

for 5 min, oven-dried at 60 °C, and then appropriately labelled (KL-1, KL-2, KL-3, MKL-1, MKL-2 or MKL-3).

3.6. Determination of the epoxy equivalent weight (EEW) of dodecyl glycidyl ether (DGE)

In this set of experiments, 2 g of DGE was added to 25 mL of 2 M pyridinium chloride (1 mL of concentrated hydrochloric acid in 61.5 mL of pyridine). The mixture was then stirred and heated to 50 °C for 30 min. After cooling the mixture, a few drops of methanol (0.1 M) and phenolphthalein were added. The solution was titrated against 0.2 M NaOH, and the blank titration was carried out as well. The EEW value of DGE was determined using equation 1 (Duraibabu et al., 2014),

$$EEW = \frac{M}{f(B-S)} \quad (1)$$

where M is the mass (g) of DGE, f is the NaOH concentration (M), B is the amount of NaOH solution (mL) utilized for the blank test, and S is the amount of NaOH solution (mL) used for dodecyl glycidyl ether sample.

3.7. NMR analysis

3.7.1. ^{1}H-NMR analysis

The DGE sample was dissolved into $CDCl_3$ with 20-30 mg/mL concentration. The solution was stirred for 30 min to fully dissolve the DGE. The ^{1}H-NMR spectrum was recorded at room temperature using an INOVA-500 MHz instrument (Varian, USA) with a 45° pulse, 32 scans and interpulse delay time of 1.0 s.

3.7.2. ^{31}P-NMR analysis

The hydroxyl groups attached to KL were quantitatively analyzed by ^{31}P-NMR, which helped identify the success of etherifying reaction (Salanti et al., 2016; Kong et al., 2015; Argyropoulos et al., 2014; Sen et al., 2013; Sadeghifar et al., 2012). The samples of KL-based material (36.6 mg) were dissolved into 500 μL of pyridine/$CDCl_3$ (1.6/1 v/v). Then, 35 μL of internal QNMR standard (21.5 mg/mL of cyclohexanol in 1.6/1 v/v pyridine/$CDCl_3$) plus 50 μL of T_1-relaxation agent (5.6 mg/mL of chromium (III) acetylacetonate in 1.6/1 v/v pyridine/$CDCl_3$) were added and the mixtures were stirred at room temperature for 40 min. Afterward, 100 μL of TMDP was added as a phosphorylating agent for the detection and quantification of phenolic and aliphatic hydroxy moieties. The reaction mixtures were stirred at room temperature for another 10 min, prior to being transferred into a 5 mm NMR tube for NMR acquisition. The NMR spectra (in the range of 200 to -20 ppm) were recorded using a INOVA-500 MHz spectrometer (Varian, USA) with a 90˚ pulse angle, 512 scans and a 5 s interpulse delay.

3.8. Phenolate and carboxylate groups analysis

The amount of phenolic hydroxyl and carboxylate groups in KL and MKL were analyzed by an automatic potentiometer (Metrohm, 728 Titrado, Switzerland), using the potentiometric titration method that was explained by Kondure et al. (2015). In this set of experiments, 0.06 g of each sample was dissolved in 1 mL of 0.8 M potassium hydroxide in a 200-mL beaker, then 4 mL of 0.5% para-hydroxybenzoic acid was added as an internal standard. Then, 100 mL of deionized water were added to the mixture, and the mixture was titrated against 0.1 M HCl standard solution to determine the content of phenolic hydroxyl and carboxylate groups (mmol/g) following equations 2 and 3,

$$\text{Phenolic hydroxyl group (mmol/g)} = \frac{[(V_2` - V_1`) - (V_2 - V_1)] \times C}{m} \qquad (2)$$

$$\text{Carboxylate group (mmol/g)} = \frac{[(V_3` - V_2`) - (V_3 - V_2)] \times C}{m} \quad (3)$$

where C is the titrant concentration (the standard solution, 0.1 M HCl), and m is the dried mass of kraft lignin (g). V_1, V_2 and V_3 are respectively the first, second and third endpoint volumes of HCl solution (mL) in the blank titration, while $V_1`$, $V_2`$, and $V_3`$ are respectively the first, second and third endpoint volumes of HCl solution (mL) used for the solution.

3.9. Elemental analysis

The organic elements of KL and MKL derivatives were assessed using an elemental analyzer (Elementar, Vario Micro, Germans). 2 mg of KL, dried at 60 °C overnight, were analyzed for their carbon, hydrogen, nitrogen, and sulfur contents by following a previously established method (Jahan et al., 2012; Fadeeva et al., 2008; Alkhalifa, 2017). An average of three independent experiments is reported.

3.10. Fourier transform infrared (FTIR) spectroscopy

To analyze the chemical structure of unmodified and modified KL, 50 mg of each sample was dried overnight at 60 °C to remove any moisture. Then, FTIR spectra were recorded using a Bruker Tensor 37, Germany, with ATR accessory. The spectra were recorded in the transmittance mode in the range of 500 cm^{-1} to 4000 cm^{-1} with resolution 1 cm^{-1} (Salanti et al., 2016). Each sample was scanned multiple times for consistency.

3.11. Charge density

A 1% suspension of different KL samples was stirred overnight at 500 rpm in a 50-mL centrifuge tube. It was then incubated for 2 h at 30 °C in a water bath shaker (Innova 3100, Brunswick Scientific, Edison, NJ, USA) and shaken at 170 rpm. The samples were centrifuged at 2000 rpm

for 5 min. The supernatant, containing the soluble component, was titrated on a particle charge detector (Mutek, PCD 04, 47 Germany) with a (0.005 M) PDADMAC standard solution. Afterward, the charge density of soluble lignin (meq/g) was determined according to equation 4 (He and Fatehi, 2015; Couch et al., 2016):

$$\text{Soluble lignin charge density } (\text{meq/g}) = \frac{\text{Volume of titrant} \times \text{Concentration of titration}}{\text{Mass of lignin}} \times \text{dilution factor} \quad (4)$$

The charge density of insoluble lignin was also measured. A 0.05 g sample of undissolved lignin from the centrifuge tube was dried and then mixed with PVSK standard solution (0.005 M). The mixture was then immersed into the water bath shaker for another two h at 30 °C and 170 rpm. Meanwhile, a blank sample was also prepared. After collecting the supernatant of each sample, the charge density of insoluble lignin was measured by determining the concentration of PVSK solutions before and after mixing with lignin samples and they were titrated against standard PDADMAC solution. The charge density of insoluble lignin (meq/g) was determined according to equation 5 (He and Fatehi, 2015; Couch et al., 2016):

$$\text{Insoluble lignin charge density } (\text{meq/g}) = \frac{(\text{Vol. PVSK for blank} - \text{Vol. PVSK for sample}) \times \text{conc. PVSK} \times \text{total mass PDADMAC}}{\text{Mass of lignin} \times \text{Mass PDADMAC}} \quad (5)$$

3.12. Solubility analysis

The solubility of the lignin samples was determined according to the method described by Konduri and Fatehi (2015). A 0.2 g lignin sample was suspended in 20 mL of deionized water to produce a 1 wt.% solution, and the samples were immersed in a water bath shaker (Innova 3100, Brunswick Scientific, Edison, NJ, USA), and stirred at 170 rpm for 2 h at 30 ˚C. The samples were then

centrifuged at 1500 rpm for 5 min to separate soluble and insoluble lignin from the mixtures, and then filtered using nylon filters (0.45 µm pore size). The filtrates were dried at 105 °C to determine their lignin concentration and thus dissolved lignin mass. The solubility of the samples was determined following equation (6):

$$\text{Solubility (wt.\%)} = \frac{\text{Mass of dissolved lignin}}{\text{Initial mass of lignin}} \times 100 \qquad (6)$$

3.13. The degree of substitution (DS)

The degree of substitution (DS) was calculated on the basis of ^{31}P-NMR quantification analysis using the following equation (7),

$$DS_{NMR} = \frac{C_f - C_i}{C_i} \qquad (7)$$

where C_f and C_i are the final and initial concentrations of hydroxyl groups in the starting material and the modified kraft lignin, respectively.

3.14. Molecular weight analysis

KL and MKL derivatives were not water-soluble. Therefore, their molecular weight determination was only possible using a static light scattering (SLS) technique. Each sample was prepared at five different concentrations (0.2. 0.4, 0.6, 0.8, and 1 g/L) in DMF solution and stirred at 500 rpm overnight. These solutions were then filtered utilizing 30 mm nylon syringe filters with a 0.45 µm pore size (Celltreat Scientific Products). The intensities of the scattered light were measured using a static light scattering instrument (Brookhaven BI-200SM, Holtsville, NY), which was attached to a goniometer at various angles between 15 ° and 155 ° and the laser wavelength was set at 637 nm. Finally, the generated data was analysed using BIC Zimm Plot software (Couch et al., 2016; Alkhalifa, 2017).

3.15. Thermal analysis (TGA and DSC)

For determining the thermal stability of kraft lignin, 8-10 mg samples were dried for two days at 60 °C to remove any moisture. Then, each sample was loaded in a platinum crucible and thermogravimetric analysis performed (i-1000 seriesTGA, Instrument Specialist Inc). Samples were heated isothermally at 100 °C, to ensure the removal of any moisture, and then at 10 °C/min to 700 °C under nitrogen (35 mL/ min) (Khazraie et al., 2017). The thermal behavior of KL derivatives was investigated with a differential scanning calorimeter (TA instrument, Q2000 DSC) using the standard cell RC mode. All samples were dried overnight at 60 ˚C prior to the DSC analyses. Approximately 10 mg of each sample was loaded into a hermetic aluminum pan and analyzed in the heat/cool/heat mode between 30 and 250 °C at a rate of 5 °C/min under 50 mL/min nitrogen flow. In the second heating cycle, the glass transition and melting point temperatures were determined (Argyropoulos et al., 2014).

3.16. Surface imaging

In this experiment, 1% solutions of each KL derivative were prepared in various solvents (water, ammonium hydroxide, and DMF), allowed to air dried for 24 h. After drying, the samples prepared as stated in section 3.17.3 was coated with gold (ERNEST F. FULLAM, INCORPORATED LATHAM, N. Y.) under vacuum (200 mTorr) for 2 min, and the images were recorded by a field emission scanning electron microscopy (FE-SEM; Hitachi Su-70).

3.17. Surface forces and wettability measurements

3.17.1. Contact angle analysis

The contact angle is determined by a combination of the intermolecular and surface forces (surface tension) and external force (gravity) (Yuan and Lee, 2013; Wang et al., 2011; Janssen et al., 2006). The contact angle analysis is defined as the angle formed by surface intersection of liquid-solid

interface in a specific environment. In Figure 3.2, a drop of liquid rests on a horizontal solid surface, which may result in three different scenarios; 1) $\theta < 90°$ indicates that the wetting of the solid surface is favorable and the wetting will increase over time over a larger surface area, 2) $\theta > 90°$ implies that the wettability of the surface is unfavorable, and 3) $\theta = 0°$ indicates a flat puddle and a complete wetting (Yuan and Lee, 2013; Fadeev and McCarthy, 1999).

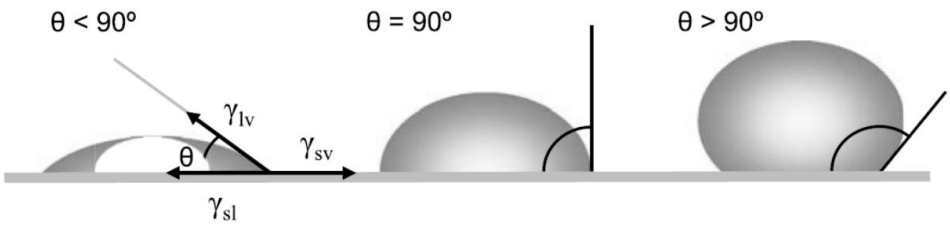

Figure 3.2. Illustration of contact angles formed by sessile liquid droplet on a smooth solid surface.

In this set of experiments, the contact angle of each lignin sample in solutions was measured using an optical tensiometer instrument, Theta lite (Biolin Scientific, Finland) equipped with a camera with sessile liquid drops on a smooth solid surface (microscopic glass slides). At first, kraft lignin sample was prepared at various concentrations (0.2, 0.4, 0.6, 0.8 and 1 g/L) in DMF by stirring at 500 rpm overnight and room temperature. It is worth mentioning that, the volume of the droplet (3 μL) and the recording time (20 seconds) were constant in all measurements. An average of three independent experiments and five droplets were considered in each experiment. The same measurements were applied on all kraft lignin and methylated kraft lignin derivatives.

3.17.2. Surface tension measurements

In a pure liquid droplet, the net force of each molecule in the bulk is zero as it is pulled equally in all directions by surrounding liquid molecules. However, this scenario is not the same for the molecule at surface. Instead, the surface molecules are pulled inward by neighboring ones causing

an internal pressure. This contraction from the molecules under the surface and from the molecules on the surface generate tension on surface of liquids. As a result, the surface tension is responsible for the shape of a liquid droplet, and could be determined by analysing its drop shape (Yuan and Lee, 2013; Mandavi et al., 2008; Janssen et al., 2006).

The surface tensions of all solutions samples were measured using an optical tensiometer instrument, Theta lite (Biolin Scientific, Finland) equipped with a camera with pendant droplet shape analysis. When a drop of liquid hanging on the needle of the instrument, its shape could be studied from the balance of forces that include the surface tension. Equation 8 is used for determining the surface tension of a droplet following the pendant drop method (Yuan and Lee, 2013):

$$\gamma = \Delta\rho g \frac{R_0^2}{\beta} \qquad (8)$$

where γ is surface tension, $\Delta\rho$ is the difference between density of phases, g is gravitational constant, R_0 is the radius of drop curvature at apex, and β is a shape factor defined by the instrument (Yuan and Lee, 2013).

In this set of experiments, each kraft lignin sample was prepared at five different concentrations (0.2, 0.4, 0.6, 0.8 and 1 g/L) to investigate the effect of the lignin concentration on the surface tension. The sample solutions were prepared at room temperature and 500 rpm in DMF. The volume of the droplet (5 µL) and the time (2 min) of analysis were constant. The same experiments were applied on all samples.

In another set of experiments, a 20 g/L concentration of kraft lignin sample was prepared at 22 °C in DMF. The droplet valume was 5 µL and the analysis was conducted for 2 min. This analysis was conducted to investigate the effect of the molar ratios of DGE/lignin on modified lignin on

the surface tension of DMF. An average of three independent experiments was conducted in this test.

3.17.3. Preparation of surfaces coated with lignin samples

Several studies were reported on how to prepare a coated layer of different lignin or starch on various substrates (Notley et al., 2006; Maximova et al., 2004; Fadeev and McCarthy, 1999; Hu T., 2002). However, the properties of the coated lignin on surfaces are affected by roughness, uniformity, or stability, causing a limitation in fundamental studies (Norgren et al., 2006). To form a thin uniform films of kraft lignin solutions on flat substrates, spin-coating is generally used. In this set of experiments, an excess amount of solutions containing kraft lignin derivatives was placed on microscopic glass slides. The substrate was then rotated at various rpm (100, 500 and 1000 rpm) using a spin coater, WS-650 (Laurell Technologies Corp) under vacuum with 60 Psi pressure to spread the fluid on the slide by the centrifugal force. Rotation was continued for 60 seconds with fluid being spun off the edges of the substrate, until the desired film was formed. Some important factors that should be considered for forming a film successfully could be the viscosity of the sample solution and solvent type, the wetting and spreading characteristics of the solvents, as well as the evaporation rate (Norgren et al., 2006). All kraft lignin and methylated kraft lignin samples were dispersed in different solvents such as dimethylformamide (DMF), water and ammonium hydroxide (NH_4OH, 0.75 M). For each lignin sample, nine substrates were prepared in three solvents (20 g/L). Three methods of natural evaporation at room temperature, heating in an oven at 60 °C and spin-coating drying at spinning rates of 100, 500 and 1000 rpm were conducted on all samples. Sodium lignosulfonate was also used as a reference. The aim of this section was to study the impact of preparation method on the surface properties of coated lignin samples. These samples were also used for SEM analysis.

For each lignin sample, 48 independent films were prepared to study different factors such as solvent (water, ammonium hydroxide, and DMF), temperature (22 °C and 60 °C), spinning rate (500 rpm, 1000 rpm), and recording time (5 s. and 20 s.).

3.17.4. Contact angle of water on coated glass slides

The contact angle of water with kraft lignin derivatives coated on microscopic slides was also measured by sessile drop method using the optical tensiometer, Theta lite (Biolin Scientific, Finland) equipped with camera (Norgren et al., 2006; Zhang et al., 2016). Approximately, 5 µL of water droplet was loaded on the microscopic slides coated with lignin samples and the contact angle between the water droplet and coated slides were determined via an optical tensiometer. In another set of experiment, a droplet of water (3 μL) was loaded on the coated films and the contact angle was recorded at different times (5 s. and 20 s.). Five replicates were performed for each sample solution and the average values were reported.

3.17.5. Interfacial tension analysis

The wettability of kraft lignin derivatives and methylated kraft lignin derivaties was determined via an optical tensiometer instrioment, Theta lite (Biolin Scientific, Finland) equipped with camera. The tensiometer's OneAttension software was utilized to measure the surface tention of kraft lignin via Zisman equation (9) (Zhu et al., 2009; Konduri, 2017).

$$\cos\theta = 1 + b\,(\gamma_{SV} - \gamma_{LV}) \qquad (9)$$

where γ_{SV} and γ_{LV} are surface tensions (mN/m) of solid (kraft lignin) and liquid (water), respectively. θ is the contact angle between the solid (kraft lignin) and liquid (water) in degrees. The cos θ is plotted against γ_{LV} yielding a straight line with slope b and γ_{SV}.

The interfacial tension between solid (kraft lignin derivatives) and water droplet was measured via utilizing Young equation (10).

$$\gamma_{LV} \cos\theta = \gamma_{SV} - \gamma_{SL} \qquad (10)$$

where γ_{LV}, γ_{SV} and γ_{SL} are the surface tensions (mN/m) of liqud vapour, solid vapour and solid liquid, respectively. The contact angle of water droplets on the kraft lignin derivatives coated slides

References

Alkhalifa, Z. 2017. Copolymerization of pretreated kraft lignin and acrylic acid to produce flocculants for suspension and solution systems. Lakehead university. Mater thesis.

Argyropoulos, D., Sadeghifar, H., Cui, C., Sen, S. 2014. Synthesis and characterization of poly(arylene ether sulfone) kraft lignin heat stable copolymers. ACS Sustainable Chemistry and Engineering, 2(2), 264-271.

Chen, C., Li, M., Wu, Y., Sun, R. 2014. Modification of lignin with dodecyl glycidyl ether and chlorosulfonic acid for preparation of anionic surfactant. RSC Advances, 4(33), 16944-16950.

Couch, R., Price, J., Fatehi, P. 2016. Production of flocculant from thermomechanical pulping lignin via nitric acid treatment. ACS Sustainable Chemistry and Engineering, 4(4), 1954-1962.

Duraibabu, D., Alagar, M., Kumar, S. 2014. Studies on mechanical, thermal and dynamic mechanical properties of functionalized nanoalumina reinforced sulphone ether linked tetraglycidyl epoxy nanocomposites. RSC Advance, 4(76), 40132-40140.

Fadeev, A., McCarthy, T. 1999. Trialkylsilane monolayers covalently attached to silicon surfaces: wettability studies indicating that molecular topography contributes to contact angle hysteresis. Langmuir, 15(11), 3759-3766.

Fadeeva, V., Tikhova, V., Nikulicheva, O. 2008. Elemental analysis of organic compounds with the use of automated CHNS analyzers. Journal of analytical chemistry, 63(11), 1094-1106.

He, W., Fatehi, P. 2015. Preparation of sulfomethylated softwood kraft lignin as a dispersant for cement admixture, RSC Advance, 5(58), 47031-47039.

Jahan, M., Liu, Z., Wang, H., Saeed, A., Ni, Y. 2012. Isolation and characterization of lignin from prehydrolysis liquor of kraft-based dissolving pulp production. Cellulose Chemistry and Technology, 46(3-4), 261-267.

Janssen, D., De Palma, R., Verlaak, S., Heremans, P., Dehaen, W. 2006. Static solvent contact angle measurements, surface free energy and wettability determination of various self-assembled monolayers on silicon dioxide. Thin Solid Films, 515(4), 1433-1438.

Khazraie, T., Zhang, Y., Tarasov, D., Gao, W., Price, J., DeMartini, N., Hupa, L., Fatehi, P. 2017. A process for producing lignin and volatile compounds from hydrolysis liquor. Biotechnology for Biofuels, 10(1), 1-14.

Konduri, M. 2017. New generation of dispersants by grafting lignin or xylan. Lakehead university. Doctoral dissertation.

Konduri, M., Fatehi, P. 2015. Production of water-soluble hardwood kraft lignin via sulfomethylation using formaldehyde and sodium sulfite. ACS Sustainable Chemistry and Engineering, 3(6), 1172-1182.

Kong, F., Wang, S., Price, J., Konduri, M., Fatehi, P. 2015. Water soluble kraft lignin–acrylic acid copolymer: synthesis and characterization. Green Chemistry, 17(8), 4355-4366.

Mandavi, R., Santosh, K., Rathore, N. 2008. Critical micelle concentration of surfactant, mixed-surfactant and polymer by different method at room temperature and its importance. Oriental Journal of Chemistry, 24(2), 559-64.

Norgren, M., Notley, S., Majtnerova, A., Gellerstedt, G. 2006. Smooth model surfaces from lignin derivatives. I. Preparation and characterization. Langmuir, 22(3), 1209-1214.

Sadeghifar, H., Cui, C., Argyropoulos, D. 2012. Toward thermoplastic lignin polymers. Part 1. Selective masking of phenolic hydroxyl groups in kraft lignins via methylation and oxypropylation chemistries. Industrial and Engineering Chemistry Research, 51(51), 16713-16720.

Salanti, A., Zoia, L., Orlandi, M. 2016. Chemical modifications of lignin for the preparation of macromers containing cyclic carbonates. Green Chemistry, 18(14), 4063-4072.

Sen, S., Sadeghifar, H., Argyropoulos, D. 2013. Kraft lignin chain extension chemistry via propargylation, oxidative coupling, and claisen rearrangement. Biomacromolecules, 14(10), 3399-3408.

Wang, J., Yao, K., Korich, A., Li, S., Ma, S., Ploehn, H., Loving, P., Wang, C., Chu, F., Tang, C. 2011. Combining renewable gum rosin and lignin: Towards hydrophobic polymer composites by controlled polymerization. Journal of Polymer Science Part A: Polymer Chemistry, 49(17), 3728-3738.

Yuan, Y., Lee, T. 2013. Contact angle and wetting properties. Surface Science Techniques, 51, 3-34.

Zhang, L., Zhang, L., Zhou, T., Wu, Y., Xu, F. 2016. The dual effects of lignin content on enzymatic hydrolysis using film composed of cellulose and lignin as a structure model. Bioresource Technology, 200, 761–769.

Zhu, R., Cui, S., Wang, X. 2009. Theoretical foundation of Zisman's empirical equation for wetting of liquids on solid surfaces. European Journal of Physics, 31(2), 251-256.

Chapter 4: Results and Discussion

4.1. Dodecyl glycidyl ether (DGE) characterization

Glycidyl ethers have been produced in various formulas via different routes as the starting materials for synthesizing alcohols (Renner et al. 1985; Zech, J., 1951; Bertram, J., 1972). Alcohols can be reacted with epichlorohydrin to generate glycidyl ethers (Rowell et al., 1994). In this work, dodecyl glycidyl ether (DGE) was prepared according to the method Chen and his coworker used (Chen et al., 2014). Scheme 4.1 shows the reaction for preparing glycidyl ethers. Epichlorohydrin was the source of epoxide ring and 1-dodecanol was chosen with aliphatic chain (12 carbons) to attach to an epoxide ring via ether bond. This alcohol was chosen with one hydroxyl group because otherwise the corresponding di and polyalcohol epoxy based products are either very high viscosity or solids and thus cannot be modified easily (Bertram, J., 1972). The reaction was carried out in steps. At first, alcohol deprotonated in the presence of the base (NaOH), then the catalyst (quaternary ammonium salt) transferred the charged derivative to the liquid where the reaction with epichlorohydrin took place. A 50 wt.% yield of the product (DGE) was obtained and a determination of epoxide weight content was followed.

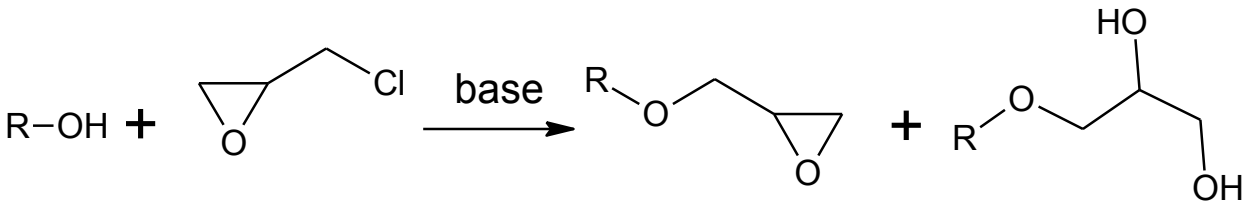

Scheme 4.1: the reaction route of epichlorohydrin and 1-dodecanol for glycidyl ethers production.

The epoxide content of DGE could be expressed in epoxide number (eq./Kg) or equivalent weight (g/mol). In the present work, Duraibabu and coworker's method (Duraibabu et al., 2014) was used to determine the epoxy value of DGE, which was 212.63 g/mol. Comparing to the theoretical value

(242.4 g/mol), it can be stated that the products contained a small amount of impurity, which contributed to the lower EEW (epoxide equivalent weight). Also, some diol may be formed as the products of side-reactions. ^{1}H NMR spectrum of the product of DGE is shown in Figure 4.1. ^{1}HNMR was used to determine the ratio of main product (DGE) to the by-product (diol), which was 1/1 molar ratio. The resonance signal of epoxide group was reported to be between 2.5 ppm to 4.5 ppm (Garea et al., 2006; Hou et al., 2000; Garcia et al., 2003; Labbé et al., 2011).

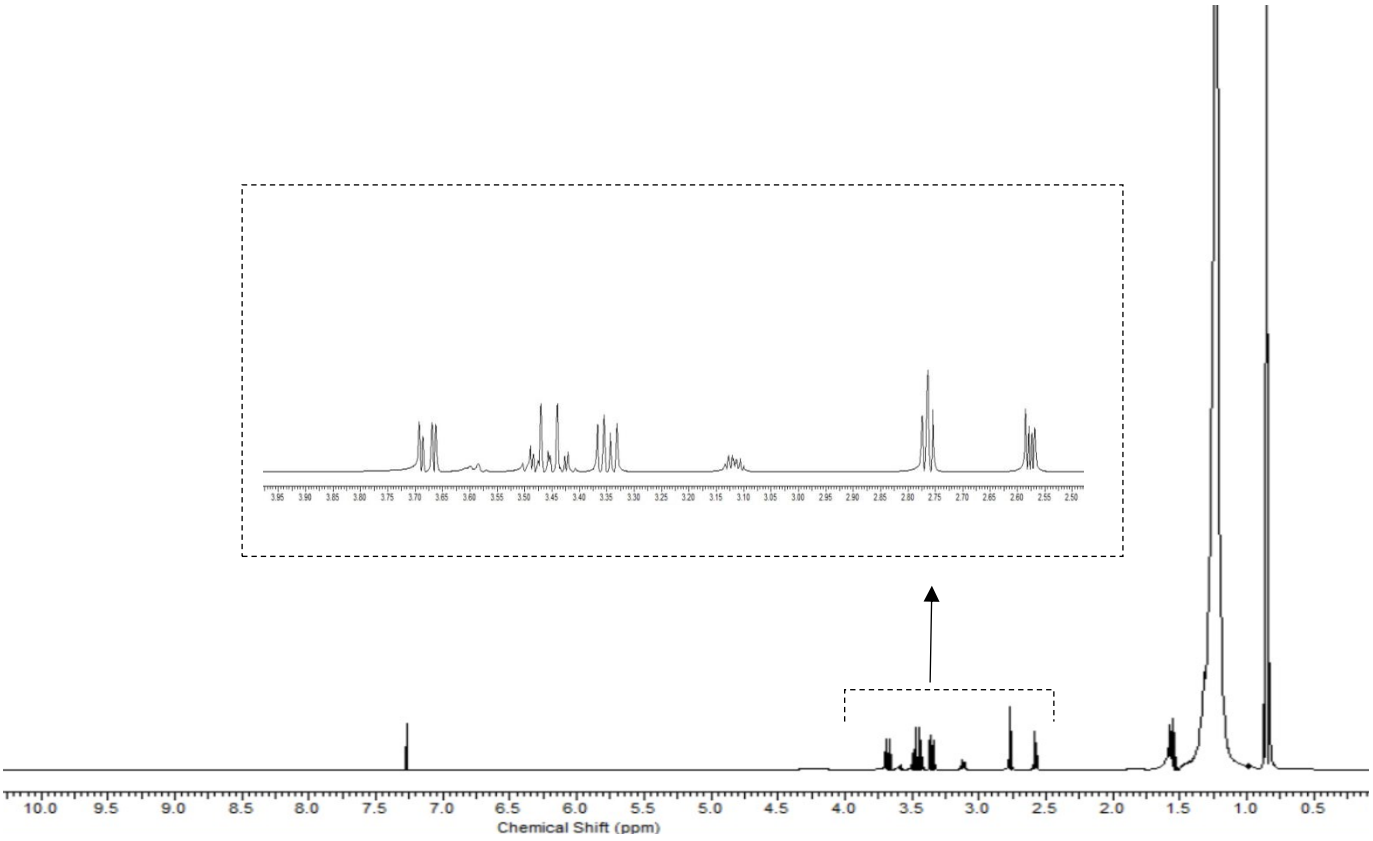

Figure 4.1: ^{1}HNMR spectrum of the DGE in $CDCl_3$

4.2. Kraft lignin pretreatment

The main objective of this work was to increase lignin's hydrophobicity by alkoxylation reaction and to study the effects of masking phenolic hydroxyl group of lignin via methylation on this modification reaction.

4.2.1. Methylation of kraft lignin

In this study, dimethyl sulfate was chosen to be the source of the methyl group because it has a high degree of hydrolysis at a high temperature (80 °C) and pH (≈11.5). Generally, when the level of methylation is high (e.g. 2.5 mmol of dimethyl sulfate per each mmol of phenolic-OH group in softwood kraft lignin), the pH should be kept at 11.5 by continuously adding NaOH to the reaction to compensate for the rapid hydrolysis of dimethyl sulfate producing sulfuric acid. The phenolic-OH group must be ionized to enable methylation and this happens under alkaline pH (Sadeghifar et al., 2012).

Scheme 4.2 shows the methylation of kraft lignin with dimethyl sulfate to mask phenolic-OH (condensed and non-condensed phenolic-OH). It was reported that the ionization efficiency of the phenolic-OH group was significantly higher (≤ 80 times) than the aliphatic OH in a low basic aqueous medium (such as a 0.7 M NaOH medium) (Sadeghifar et al., 2012). Thus, the methylation was conducted in this basic aqueous medium. At a high pH, the hydroxyl group in lignin are converted to sodium phenolate (alkoxide salts) before further conversion to anisole to make the reaction site more reactive. Masking degrees of phenolic-OHs group could be controlled by the molar ratio of dimethyl sulfate/lignin.

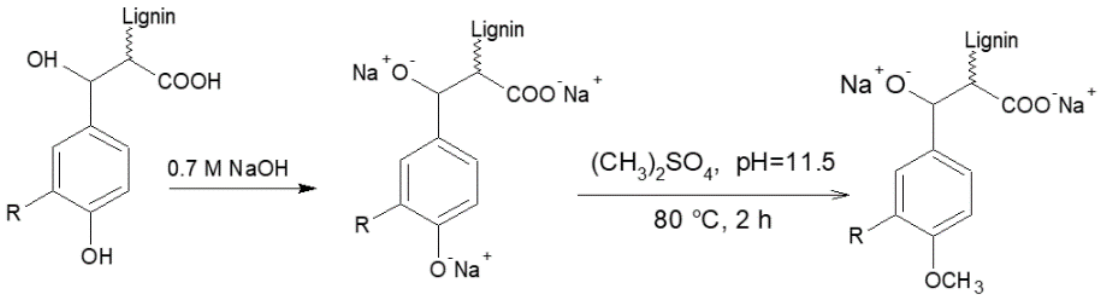

Scheme 4.2: The reaction route for methylation of kraft lignin

Kraft lignin was modified under different reaction conditions of methylation in the literature (Sadeghifar et al., 2012; Sen et al., 2015; Sen et al., 2013; Argyropoulos et al., 2014). Figure 4.2 shows the ^{31}P NMR spectrum of kraft lignin (KL) and methylated kraft lignin (MKL) in pyridine/$CDCl_3$ mixture (1.6/1 v/v). The phosphitylating agent (2-chloro-4,4,5,5- tetramethyl-1,2,3-dioxaphospholane) was used to obtain the qualitative and quantitative information about hydroxyl groups in kraft lignin before and after grafting with DGE. The peaks appeared in the range of 150.0 ppm and145.4 ppm belong to aliphatic-OH groups. The peaks appeared at 144.5 ppm – 137.0 ppm range are associated with phenolic-OH groups (Argyropoulos et al., 2014).

Kraft lignin

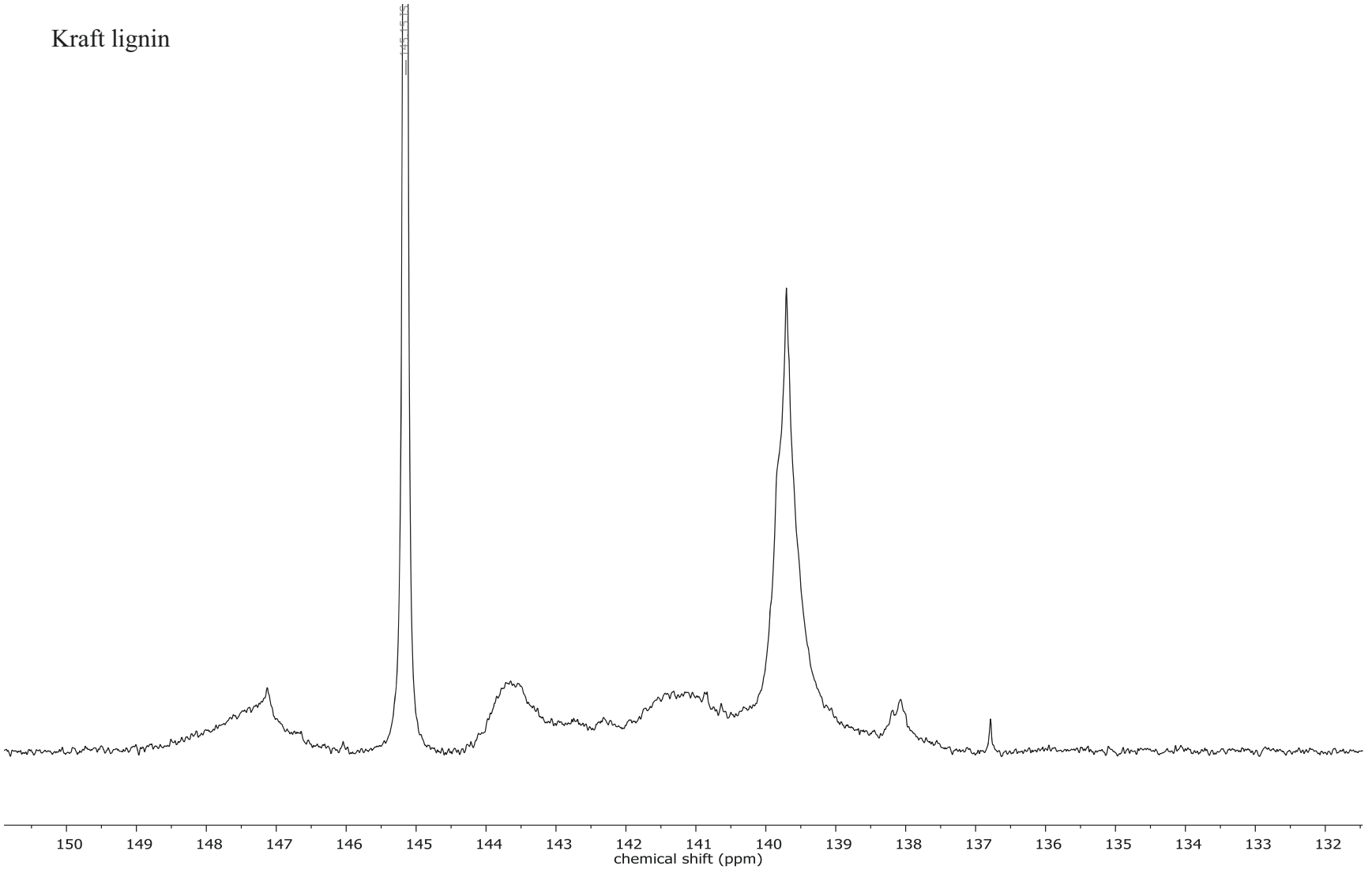

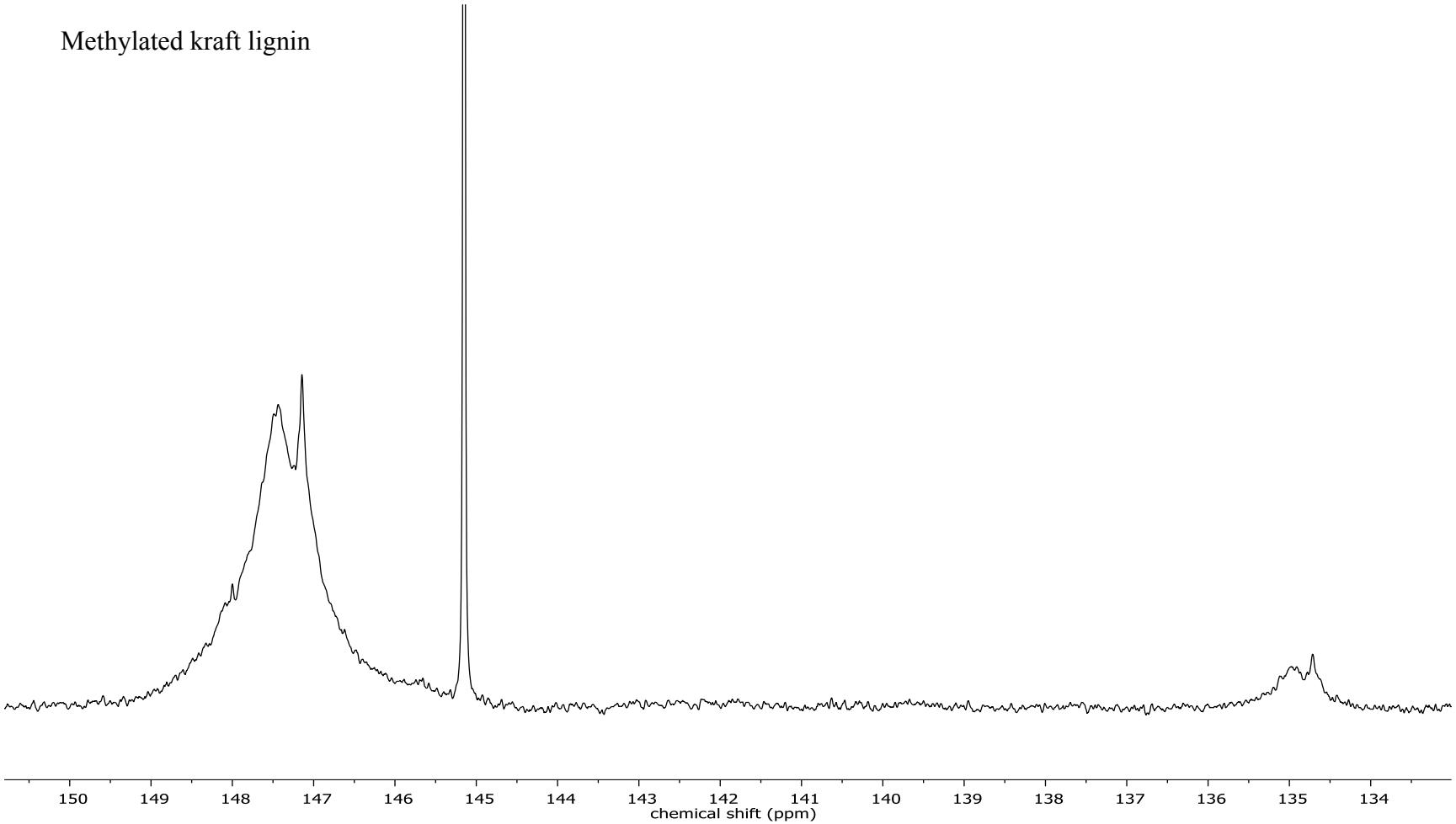

Figure 4.2: Quantitative ^{31}PNMR spectrum of kraft lignin (KL) and methylated kraft lignin (MKL) in pyridine/$CDCl_3$ mixture (1.6/1 v/v).

The areas under the peaks in Figure 4.2 were considered for quantifying the group contents attached to the lignin samples. Table 4.1 lists the mass of these groups. It is seen that the phenolic –OHs (condensed and non-condensed) peaks were significantly decreased from 0.47 mmol/g and 0.68 mmol/g to 0.06 mmol/g and 0.08 mmol/g, respectively, due to the methylation. Condensed phenolic –OHs are defined as those that belong to aromatic groups but have a substituent in the 5th carbon position in the aromatic ring, while non-condensed phenolic –OHs have no such substituents. It was reported that the reaction rate of the non-condensed phenolic –OH groups was faster than that of the condensed phenolic –OH groups in lignin structure (Sadeghifar et al., 2012; Sen et al., 2013). The low reactivity of the condensed phenolic hydroxy groups is due to the sterically hindered environment of the condensed phenolic –OHs (Sen et al., 2013). The electron donating effect of ether groups or methylene groups (through the mesomeric effect or through positive inductive effect) most likely increased the nucleophilicity of the phenoxide ions. Moreover, the existence of these groups (ether groups or methylene groups) on neighboring carbon could provide to condensed phenolic –OHs the rotational freedom that increased the accessibility and reactivity of these groups (Sen et al., 2015). Therefore, the combination of sterically and electronically favorable consideration likely made non-condensed phenolic-OH groups relatively reactive (Sen et al., 2013; Argyropoulos et al., 2014).

Table 4.1: The hydroxyl content analysis of KL and MKL by an automatic potentiometric titrator and ^{31}PNMR.

	^{31}P NMR			
Groups	KL		MKL	
	mmol/g	**%**	mmol/g	**%**
Aliphatic	0.21	14.1	1.36	83.8

Condensed	0.47	31.7	0.06	3.5
Non-condensed	0.68	45.9	0.08	5.2
Carboxylic	0.12	8.1	0.12	7.5
	Titration			
	KL (mmol/g)		MKL (mmol/g)	
Phenolic-OH	1.20 (∓ 0.1)		0.12 (∓ 0.1)	
Aliphatic-OH	0.35 (∓ 0.1)		0.33 (∓ 0.12)	

Both titration and NMR analyses confirmed that phenolic -OH were significantly decreased after methylation, which implies the success of converting phenolic -OH to methoxide (OCH_3). The remaining phenolic -OH were probably not accessible to dimethyl sulfite for the methylation reaction (e.g. via steric hindrance). As NMR is a proportional based analysis, the decrease in the phenolic -OH led to an increase in aliphatic -OH (Table 4.1). In titration analysis, the aliphatic-OHs were not affected by the methylation reaction, which confirmed that the selectivity of methylation toward the phenolic -OHs was high. Moreover, the great reduction in the phenolic-OHs indicated that the phenolic hydroxide groups were successfully converted to methoxide groups. As the quantitative ^{31}P NMR data showed that about 87.5 % of the phenolic hydroxyl groups were converted to methoxy groups in MKL production (Table 4.1). It is also seen that the methylation enhanced the carboxylate content of lignin, which might be due to the conversion of hydroxy groups to sodium phenolate in the first step of the reaction.

Figure 4.3 shows the FT-IR spectra of KL and MKL. The broad peak between 3200 and 3700 cm^{-1} correspond to O–H stretching of the hydroxyl groups. This peak became weak in MKL. Simultaneously, the C–H stretching (between 2800 and 3200 cm^{-1}) and C–O–C (at 1168 cm^{-1}) peaks slightly increased after methylation reaction. Therefore, it is evident that during the reaction

of kraft lignin with dimethyl sulfate, its phenolic hydroxyl groups were converted to the corresponding methoxy groups as the CH stretching was increased in the MKL (between 2800 and 3200 cm^{-1}). The FT-IR analysis also confirmed the success of methylation reaction.

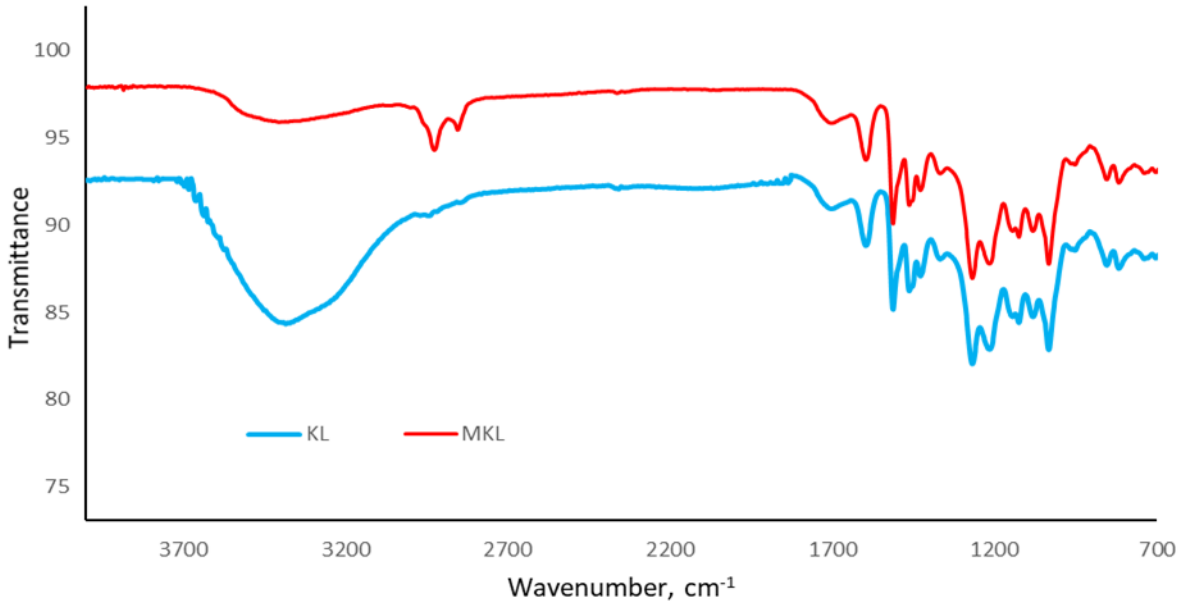

Figure 4.3: FT-IR spectrum of MKL and KL.

Table 4.2 lists the organic contents of KL and MKL. It is seen that the amount of carbon and hydrogen increased, but oxygen and sulfur decreased. These changes were attributed to the conversion of hydroxide groups to methoxide ones, while the impurity of kraft lignin such as salts was the cause of the oxygen' and sulfur's minor reductions. Based on these results, the chemical formula (on a basis of 9 carbons of repeating units) of KL and MKL can be C_9 $H_{9.84}$ $O_{3.08}$ $S_{0.06}$ and C_9 $H_{9.81}$ $O_{2.75}$ $S_{0.05}$, respectively.

Table 4.2: The elemental composition and molar mass of KL and MKL.

Sample	**Elemental analysis (wt.%)**				**Mw (g/mol)**	**C_9 Formula**
	C	H	O[a]	S		

KL	63.75	5.81	29.17	1.26	$(1.13\pm0.15)\times10^6$	$C_9H_{9.84}O_{3.08}S_{0.06}$
MKL	65.94	5.99	26.94	1.13	$(3.09\pm0.16)\times10^6$	$C_9H_{9.81}O_{2.75}S_{0.05}$

a: by difference

4.3. Reaction of kraft lignin and DGE

A series of six samples were prepared with different molar ratios of DGE to lignin's hydroxy content in DMSO at 100 °C for 5 h with both KL and MKL as starting materials. Typically, the reaction between epoxide ring and the hydroxyl groups in kraft lignin molecules can be accelerated by the addition of Lewis bases (Tänzer et al., 1993). Therefore, dimethylbenzylamine was used as the catalyst for DGE incorporation given the low reactivity of kraft lignin. The synthesis of kraft lignin and DGE is shown in Scheme 4.3. The epoxide ring reacts with the catalyst (tertiary amine) to form a zwitterion (due to its high basicity), which then reacts with the hydroxyl groups of lignin. The molar ratio of DGE/lignin was 0.348, 0.466 and 0.937 to produce KL-1, KL-2 and KL-3, respectively. The same ratios were used to produce MKL-1, MKL-2 and MKL-3.

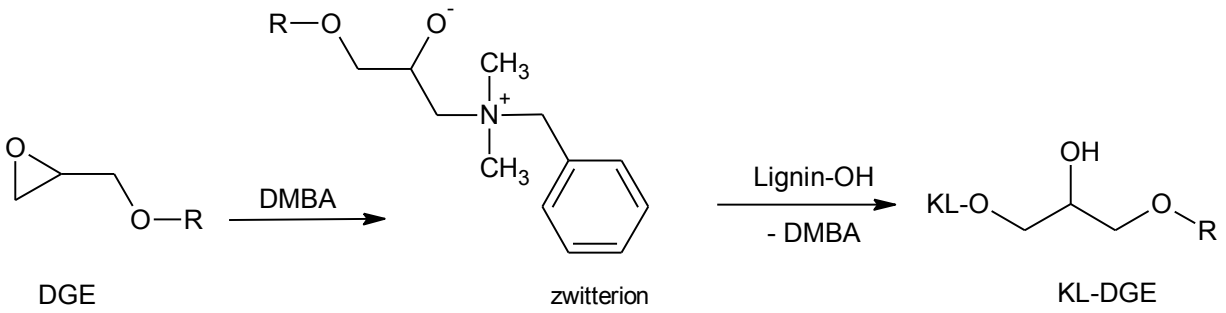

Scheme 4.3: reaction of lignin and DGE in the presence of DMBA, where R= CH_2-$(CH_2)_{10}$-CH_3.

Based on this reaction mechanism, the following phenomena can be hypothesized:

1) carboxylic-OH groups may react preferentially (compared to phenolic-OH) with DGE because of their relatively high acidity;

2) by increasing the ratio of DGE/lignin, the amount of aromatic-OH in lignin would be decreased;

3) there would be new aliphatic-OH groups derived from the open ring reaction of the epoxy group of DGE; and

4) by increasing the ratio of DGE/lignin, the products' hydrophilicity would be decreased.

4.3.1. Structural analysis of KL-DGE product

The products of KL and DGE reactions were characterized by ^{31}P-NMR in Figure 4.4 for KL, KL-1, KL-2 and KL-3 (Chen et al., 2014).

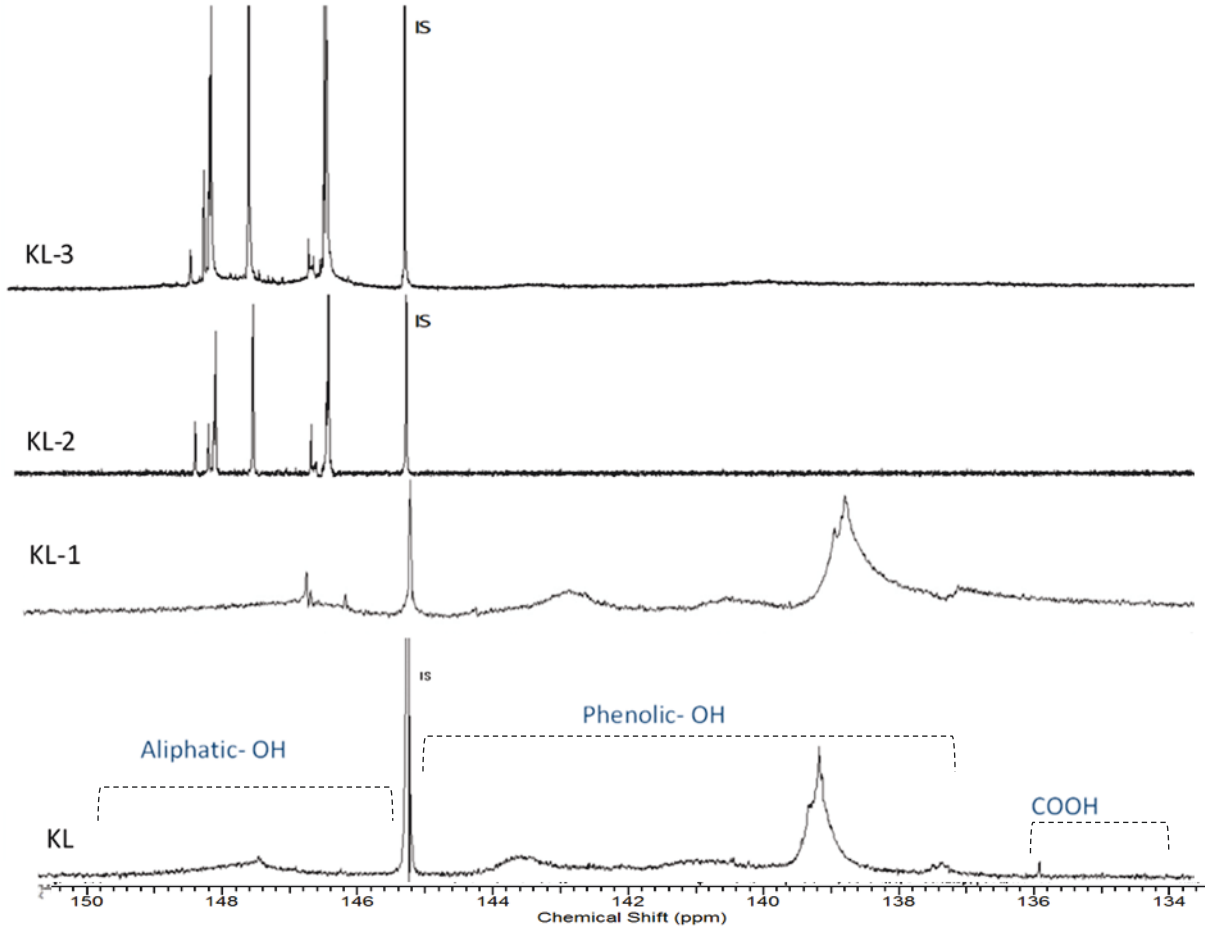

Figure 4.4: ^{31}PNMR spectrum of KL, KL-1, KL-2 and KL-3. in pyridine/$CDCl_3$ mixture (1.6/1 v/v), IS: internal standard.

According to the literature (Samuel et al., 2014), the assigned peaks for aliphatic –OH, phenolic-OH, and carboxylic –OH in kraft lignin are in the range of 150.0–145.4 ppm, 144.5–137.0 ppm, and 136.0–134.0 ppm, respectively. Indeed, three new peaks in the aliphatic –OH range were noticed (147.9–147.4, 147.1–146.8, and 146.6–145.8 ppm) in the spectra of KL-1, KL-2 and KL-3, the magnitude of which increased as the DGE/lignin molar ratio was increased. Overall, these results confirmed that DGE group was introduced to KL.

Based on these results, the amount of hydroxyl group on lignin samples are listed in Table 4.3. It is seen that the carboxylic –OH peak in KL was diminished, whereas the amount of aliphatic –OH

increased, supporting the first hypothesis that DGE reacted preferentially with carboxylic –OH groups. The loss of carboxylic –OH could explain the different charge density and water solubility of the lignin derivatives. By increasing the DGE/lignin ratio, the amounts of phenolic –OH (condensed and non-condensed) group decreased, while that of aliphatic OH increased from 0.21 mmol/g in KL to 1.48 in KL-3. However, the total OH content is unchanged suggesting that one type of OH is converted to the other types. The variation between KL-2 and KL-3 is small (Table 4.3), which is likely due to the fact that most of the phenolic –OH were converted at the lower DGE/lignin ratio. Overall, from the quantitative ^{31}P NMR data (Table 4.3), the degree of substitution (DS_{NMR}) was determined. The DS_{NMR} is increasing via raising the ratio of DGE/lignin, as KL-1, KL-2 and KL-3 display DS_{NMR} of 0.22, 1.90 and 2.01, respectively.

Table 4.3: Quantification of hydroxyl groups of KL before and after reaction with DGE using ^{31}PNMR.

Samples	**Hydroxyl content (mmol/g of KL)**				**DS_{NMR}**
	Phenolic-OH	Aliphatic-OH	Carboxylic-OH	Total OH	
KL	1.15	0.21	0.12	1.48	-
KL-1	1.13	0.35	ND	1.48	0.22
KL-2	0.08	1.41	ND	1.49	1.90
KL-3	ND	1.48	ND	1.48	2.01

ND: not detected

The degree of substitution was also measured based on NMR quantification analysis the results were shown in Table 4.3. The aliphatic chain (DGE) grafting to kraft lignin increased by increasing the molar ratios, confirming the success of this reaction.

Moreover, the products of KL and DGE reactions were analyzed for their organic contents by the elemental analyzer (Table 4.4). It is seen that the carbon and hydrogen contents of the product increased, but its oxygen and sulfur decreased as the ratio of DGE/lignin increased as a result of DGE attachment to KL. The chemical formulas for KL-1, KL-2 and KL-3 are C_9 $H_{10.11}$ $O_{2.51}$ $S_{0.1}$, C_9 $H_{11.52}$ $O_{2.46}$ $S_{0.04}$, and C_9 $H_{11.66}$ $O_{2.46}$ $S_{0.04}$, respectively, compared to C_9 $H_{9.84}$ $O_{3.08}$ $S_{0.06}$ for the original kraft lignin. Similar to the ^{31}P-NMR analysis, there was only a small difference between the chemical formulas of KL-2 and KL-3.

As listed in Table 4.4, the molecular weight of KL-1, KL-2 and KL-3 increased as the ratio of DGE/KL increased. The general trend supports the fact that grafting DGE to kraft lignin increased the molecular weight of lignin. At a lower DGE/KL ratio, DGE might only attach to OH of carboxylate group, as the reaction between carboxyl and glycidyl ether occurred first due to the relatively high acidity of carboxyl in lignin (Chen et al., 2014). However, at a higher DGE/KL ratio, DGE was also grafted to lignin at phenolic –OH reactive site leading to a reduction in phenolic –OHs concentration and an increase in the molecular weight.

Table 4.4: The characteristics of KL-DGE product.

Sample	Elemental analysis (wt. %)				Mw (g/mol)	C_9 Formula	C_9 Formula-DGE
	C	H	O[a]	S			
KL	63.75	5.81	29.17	1.26	$(1.1\pm0.1)\times10^6$	C_9 $H_{9.84}$ $O_{3.08}$ $S_{0.06}$	-
KL-1	66.71	6.25	24.90	2.14	$(5.5\pm3.6)\times10^6$	C_9 $H_{10.11}$ $O_{2.51}$ $S_{0.1}$	C_9 $H_{9.62}$ $O_{3.08}$ $S_{0.06}$. 0.22 $C_{15}H_{30}O_2$
KL-2	67.28	7.18	24.59	0.93	$(1.8\pm2.1)\times10^7$	C_9 $H_{11.52}$ $O_{2.46}$ $S_{0.04}$	C_9 $H_{7.94}$ $O_{3.08}$ $S_{0.06}$. 1.90$C_{15}H_{30}O_2$
KL-3	67.32	7.27	24.54	0.86	$(4.1\pm0.3)\times10^7$	C_9 $H_{11.66}$ $O_{2.46}$ $S_{0.04}$	C_9 $H_{7.83}$ $O_{3.08}$ $S_{0.06}$. 2.01$C_{15}H_{30}O_2$

a: by difference

The FT-IR spectra of KL, KL-1, KL-2 and KL-3 are shown in Figure 4.5. According to the literature (Gan et al., 2013; Konduri, 2017), the stretching bond between 3400 and 3100 cm^{-1} corresponds to the O–H bond of aliphatic hydroxyl and phenolic hydroxyl groups, while the absorption peaks at 2930 cm^{-1} and 2300 cm^{-1} correspond to C–H and C=C stretches of aldehyde groups (Gan et al., 2013; Konduri, 2017). A comparison between the KL samples indicates that there is a noticeable decrease in the stretching bond between 3400 and 3100 cm^{-1}, which may be due to reduced carboxylic– or phenolic –OH content of KL after DGE attachment. The increase in the intensity of absorption peaks at 2924 and 2853 cm^{-1} is likely due to the introduction of long alkyl chain to KL via DGE reaction, thereby supporting the conclusion that the DGE was introduced to KL.

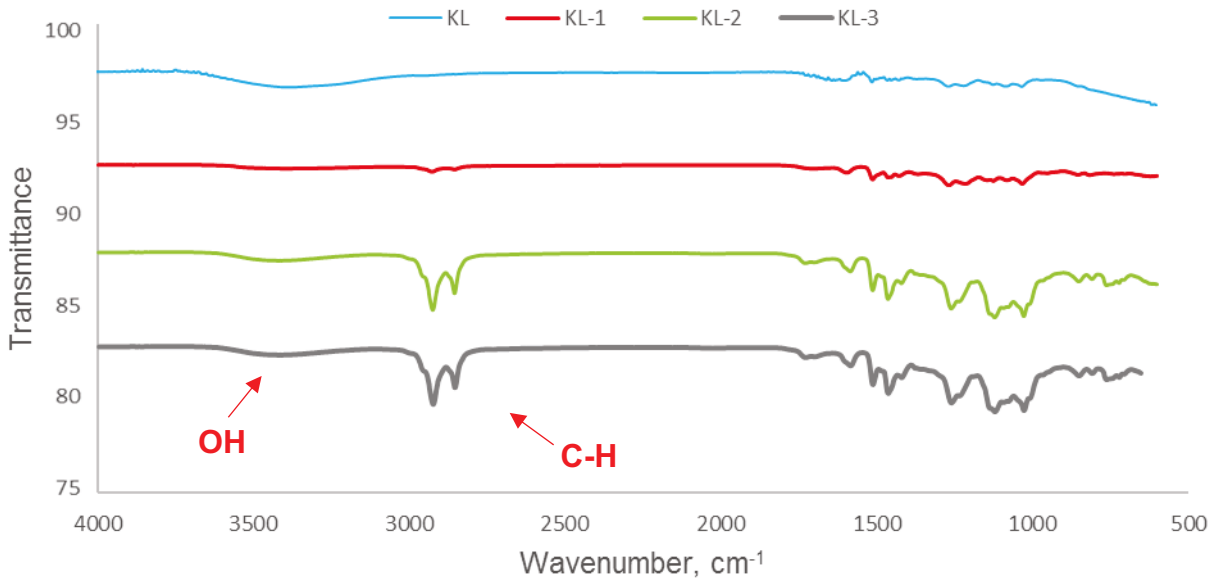

Figure 4.5: FT-IR spectra of KL, KL-1, KL-2, and KL-3.

4.3.2. Structural analysis of MKL-DGE products

The ^{31}P-NMR spectra of the products of MKL and DGE (for MKL-1, MKL-2 and MKL-3) are shown in Figure 4.6. Similar to the product of KL and DGE, the carboxylic –OH peak seen in MKL (unreacted lignin), is absent in MKL-1. With the increase in the DGE/MKL ratio, the amount of the aliphatic –OH was increased. However, the spectra of MKL-2 and MKL-3 were similar indicating that most of the remaining hydroxyl groups were converted to aliphatic –OH at the lower molar ratio for MK-1 production. As expected, the phenolic –OH signal is absent in MKL, as it was converted in the methylation reaction.

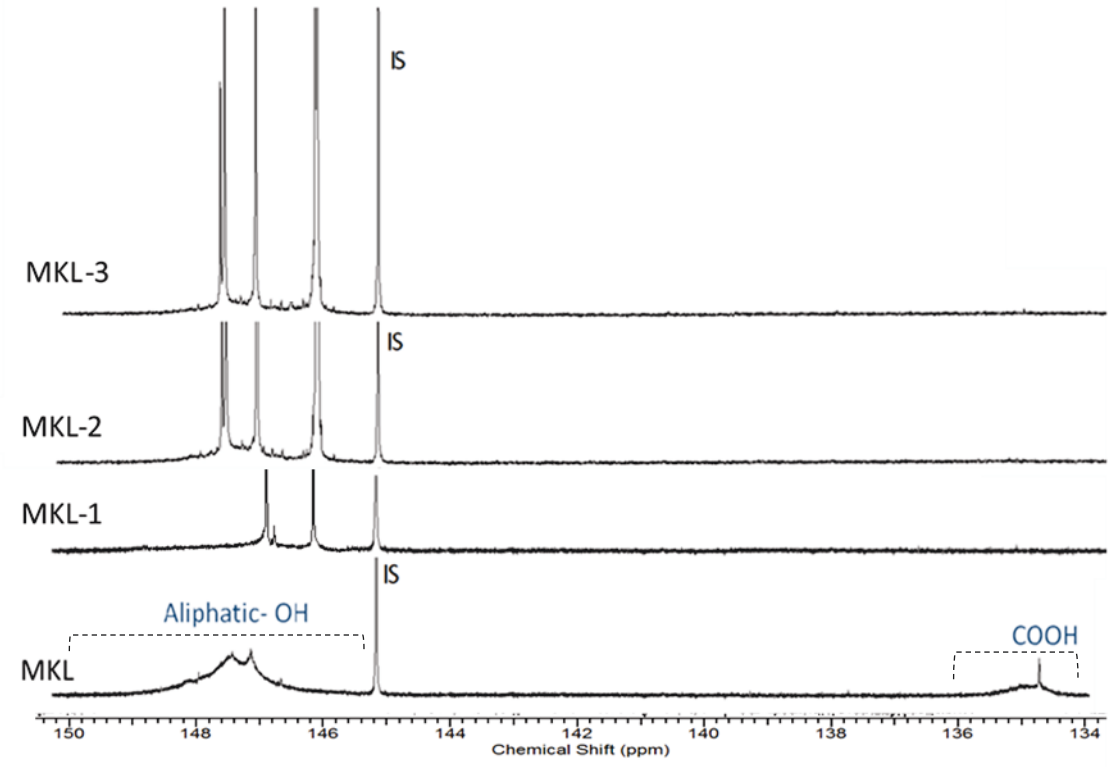

Figure 4.6: ^{31}PNMR spectra of MKL, MKL-1, MKL-2 and MKL-3 in pyridine/$CDCl_3$ mixture (1.6/1 v/v) IS: internal standard.

In Table 4.5, the DS in methylated kraft lignin was increased by increasing the molar ratio from 0.07 to 1.13. Also, the number of reactive sites in methylated samples were lower than the ones in kraft lignin due to the methylation pretreatment.

MKL based products were analyzed by the CHNS analyzer to investigate its organic elements and the results are available in Table 4.5. The carbon and hydrogen contents of MKL were increased, while its hydrogen and oxygen decreased as a result of DGE grafting onto MKL. Furthermore, the carbon content was higher in MKL-1, MKL-2 and MKL-3 (C_9 $H_{10.98}$ $O_{2.51}$ $S_{0.03}$, C_9 $H_{11.03}$ $O_{2.40}$ $S_{0.03}$, and C_9 $H_{11.17}$ $O_{2.25}$ $S_{0.05}$, respectively) than in MKL (C_9 $H_{9.81}$ $O_{2.75}$ $S_{0.05}$). The degree of substitution was shown in table 4.5. Based on the quantitative ^{31}P NMR data, the degree of grafting DGE into methylated samples are 0.07, 0.56 and 1.13 for MKL-1, MKL-2 and MKL-3, respectively. Interestingly, the DS_{NMR} in methylated lignins was lower than unmodified lignin samples which show a great agreement with the results show in Figure 4.2 and Table 4.1, phenolic -OHs reduction. Furthermore, the molecular weight of MKL increased as its DGE amount increased.

Table 4.5: the characteristics of methylated kraft lignin based products.

Sample	Elemental analysis (wt. %)				Mw (g/mol)	DS_{NMR}	C_9 formula	C_9 Formula-DGE
	C	H	O[a]	S				
MKL	65.94	5.99	26.94	1.13	$(3.09\pm0.16)\times10^6$	-	C_9 $H_{9.81}$ $O_{2.75}$ $S_{0.05}$	-
MKL-1	67.43	6.86	25.10	0.60	$(2.36\pm0.47)\times10^6$	0.07	C_9 $H_{10.98}$ $O_{2.51}$ $S_{0.03}$	C_9 $H_{9.74}$ $O_{2.75}$ $S_{0.05}$ .0.07$C_{15}H_{30}O_2$
MKL-2	68.04	6.95	24.24	0.76	$(1.43\pm0.84)\times10^7$	0.56	C_9 $H_{11.03}$ $O_{2.40}$ $S_{0.03}$	C_9 $H_{9.25}$ $O_{2.75}$ $S_{0.05}$ .0.56$C_{15}H_{30}O_2$
MKL-3	68.81	7.12	22.98	1.08	$(4.50\pm4.10)\times10^7$	1.13	C_9 $H_{11.17}$ $O_{2.25}$ $S_{0.05}$	C_9 $H_{8.68}$ $O_{2.75}$ $S_{0.05}$ .1.13$C_{15}H_{30}O_2$

a: by difference

The FT-IR spectra of MKL, MKL-1, MKL-2 and MKL-3 are shown in Figure 4.7. Generally, the results support those of Figure 4.5. The O–H bond stretch between 3400 and 3100 cm^{-1} slightly increased for modified MKLs. The absorption at 2924 and 2853 cm^{-1} was also increased due to long alkyl chain introduction to MKL-1 MKL-2 and MKL-3.

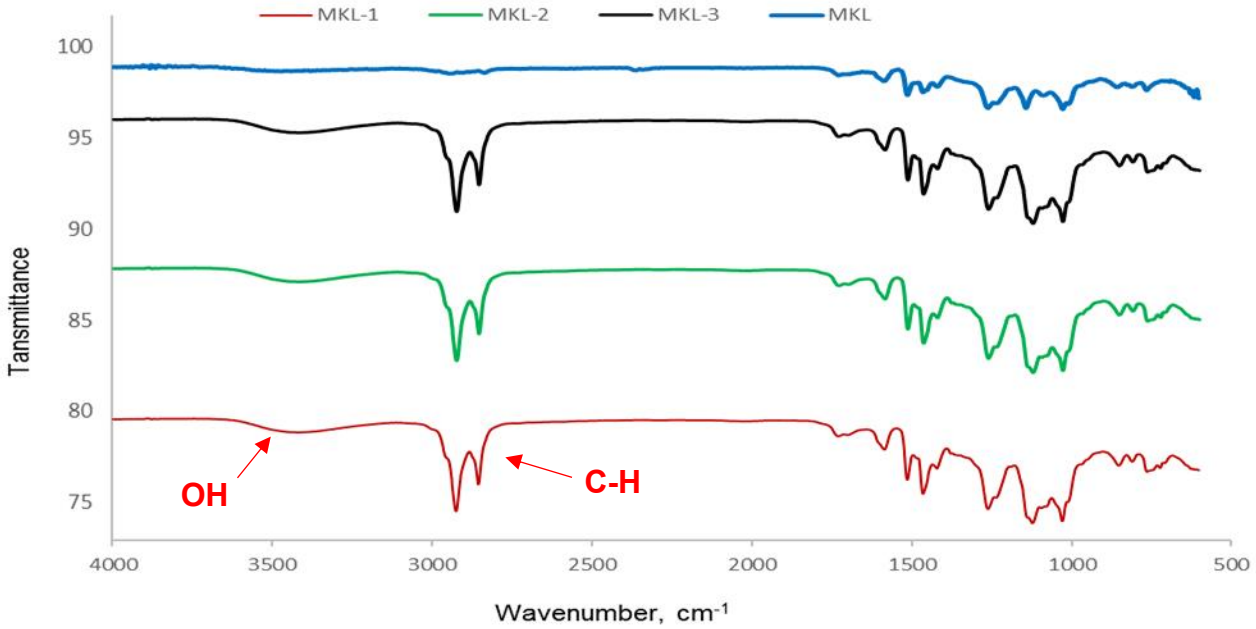

Figure 4.7: FT-IR spectra of MKL, MKL-1, MKL-2, and MKL-3.

The aforementioned results are supportive of the hypothesis that reaction of MKL and DGE (scheme 4.3) increased aliphatic –OH groups and by increasing the DGE/lignin ration, the grafted ratio increased (hypothesis 2).

4.4. Kraft lignin and lignosulfonate properties

The properties of kraft lignin and lignosulfonate are listed in Table 4.6. The molecular weight and charge density of kraft lignin were found to be 35000 g/mol and 0.29 meq/g respectively. However, lignosulfonate (LS) exhibited a higher charge density (3.13 meq/g) and molecular weight (52000 g/mol) compared to kraft lignin. High pH (10.4) of kraft lignins solution represents the presence

of some salts as impurities. The lignosulfonate is 100% water soluble with 62.5 mN/m and 19.7 g/L of surface tension and critical micelle concentration, respectively. On the other hand, kraft lignin has no effect on the surface tension of water and thus did not exhibited any CMC.

Table 4.6: Properties of kraft lignin and lignosulfonate.

Lignin	Mw (g/mol)	Solubility in water (%)	CDSL (meq/g)	Concentration (g/L)	pH	Density (g/cm3)	CMC (g/L)	ST (mN/m)
LS	52,000	100	3.13	10	5.7	0.99	19.7	62.5
KL	35,000	46	0.29	10	10.38	1.01	NA	NA

CDSL: Charge density of soluble lignin, Mw: molecular weight, CMC: critical micelle concentration, ST: surface tension, NA; not applicable.

4.5. Thermal behavior of lignin samples

4.5.1. Thermogravimetric (TGA) Analysis

Figures 4.8 and 4.9 shows the results for TGA analysis of lignin samples. Compared to KL, modified kraft lignin samples exhibited low thermal stability. Interestingly, the modified lignin samples displayed similar thermal degradation pattern irrespective of their methylation pretreatment. The weight loss below 100 °C is attributed to the elimination of moisture in all samples. The lignin samples started to decompose at a temperature higher than 200 ºC. Brebu and coworkers (2010) also reported that, the lignin degradation started between 230 ºC and 260 ºC, which was attributed to the decomposition of propanoid side chain in lignin (Brebu et al., 2010). It is observed that KL-1 had a decomposition peak below 200 ºC (Figure 4.9), however, by increasing grafting, the degradation temperature risen to higher temperatures, which is due to the replacement of hydroxyls groups by DGE reducing the number of hydrogen bonding in lignin

molecule where the first step of decomposition occurred (Laurichesse et al., 2014). According to the literature, the weight loss rate of lignin between 440 and 500°C was ascribed to the breakdown of intermolecular bonding within lignin (Zhang et al., 2014; Alkhalifa, Z. 2017).

Modified kraft lignins exhibited lower thermal resistance than unmodified lignins, and this less stability of modified lignin is attributed to the decomposition of alkyl chains (Brebu et al., 2010). The decrease in the thermal stability of lignin could be a disadvantage for its end-use applications (Wu et al., 2012).

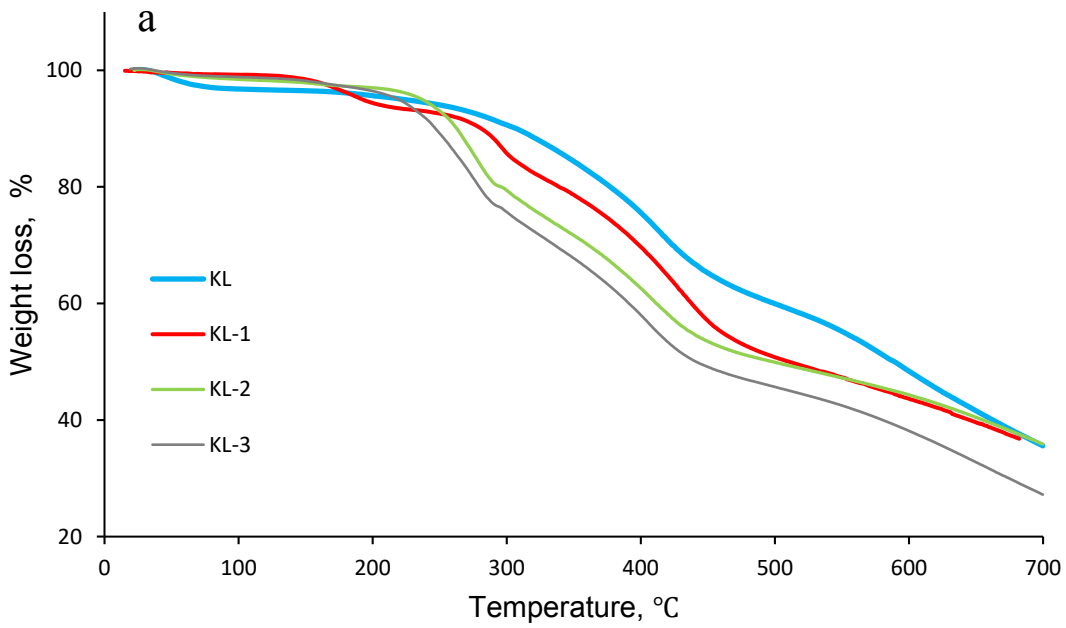

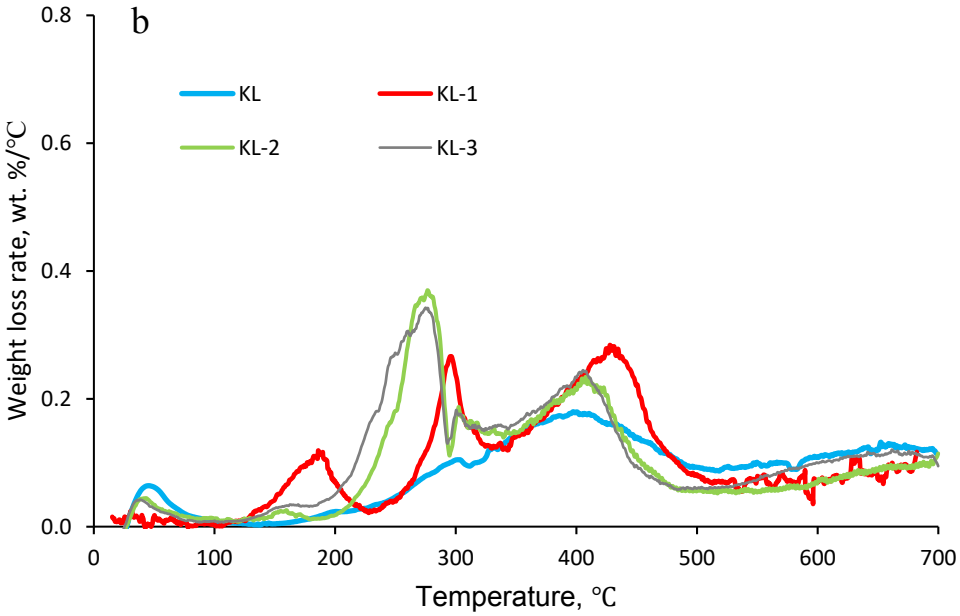

Figure 4.8: a) Weight loss and b) weight loss rate of KL, KL-1, KL-2 and KL-3 conducted under N_2 at a flow rate of 30 mL/min with heating rate of 10 ℃/min.

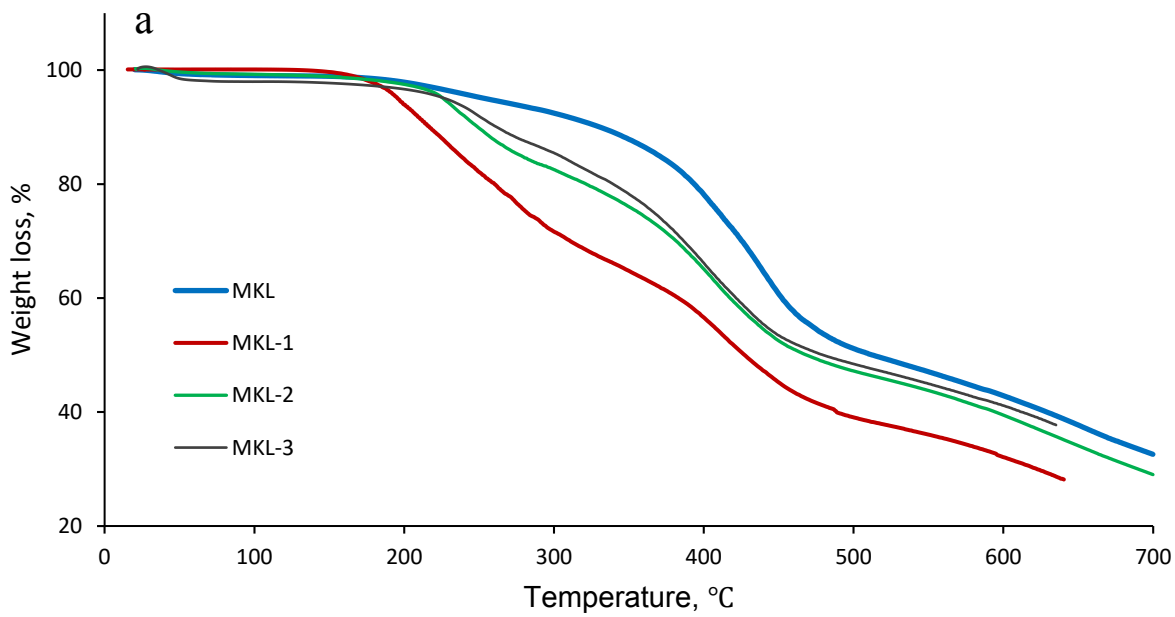

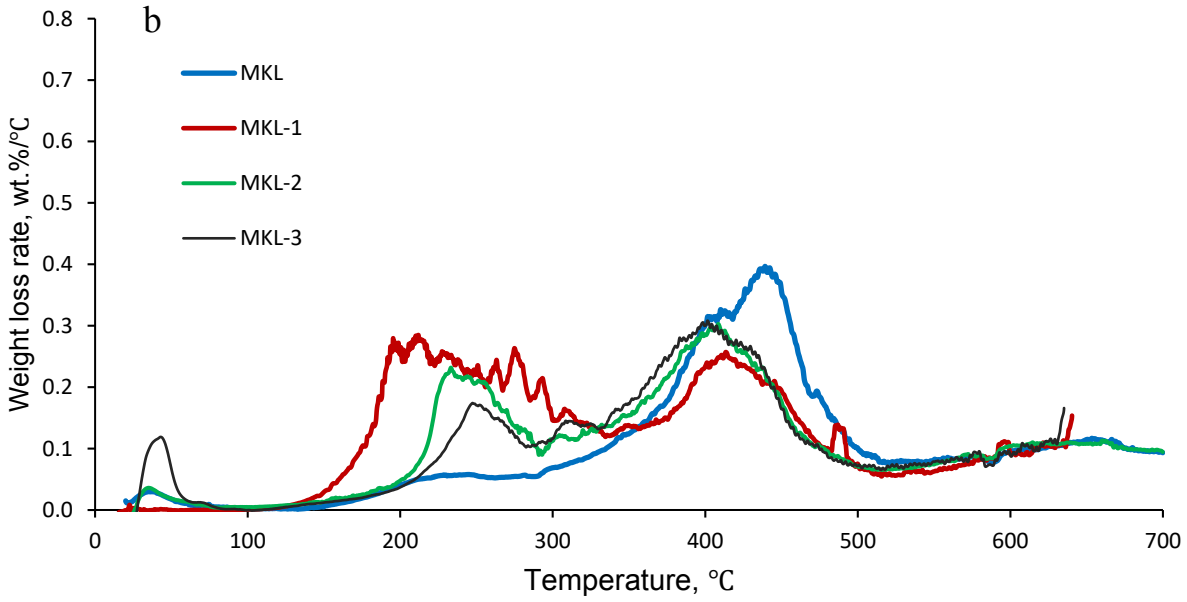

Figure 4.9: a) Weight loss and b) weight loss rate of MKL, MKl-1, MKL-2and MKL-3 conducted under N_2 at a flow rate of 30 mL/min heated at 10 °C/min.

Table 4.7 lists the thermal degradation temperatures of lignin samples derived from TGA analysis. The temperature at which 10% of weight loss occurred ($T_{10\%}$) was found to decrease significantly by increasing the ratio of DGE/lignin ($T_{10\%}$= 307, 280, 260 and 246 °C for KL, KL-1, KL-2 and KL-3, respectively). Similarly, 50% of the mass loss occurred at markedly lower temperatures compared to unmodified kraft lignin. Furthermore, by increasing the molar ratio of DGE/lignin, ash content of lignin samples dropped. The results for methylated samples followed similar trends.

Table 4.7; Thermal degradation temperatures at 10% ($T_{10\%}$) and 50% ($T_{50\%}$) weight loss of lignin samples, and ash content of lignin samples left at 700 °C (R_{700}).

Samples	**$T_{10\%}$ (°C)**	**$T_{50\%}$ (°C)**	**R_{700} (wt.%)**

KL	307	589	35
KL-1	280	510	36
KL-2	260	498	35
KL-3	246	441	27
MKL	330	512	32
MKL-1	261	479	28
MKL-2	249	468	29
MKL-3	216	447	37

4.5.2. Differential scanning calorimetry (DSC) analysis

To investigate the changes in thermal behavior of kraft lignin derivatives, the glass transition temperature, T_g, of the samples was analyzed and the results are represented in Table 4.8. As reported previously (Passoni et al., 2016; Laurichesse et al., 2014), the T_g of lignin vary depending on the type of lignin and the process lignin is produced. The T_g of kraft lignin is usually in the range between 90 and 170 °C. As shown in Table 4.8, the T_g of kraft lignin was found to be 154.33 °C. Interestingly, grafting aliphatic chain (DGE) to kraft lignin reduced the T_g values with KL-1, KL-2 and KL-3 exhibiting T_g values of 116.82 °C, 89.23 °C and 70.19 °C, respectively. Grafting DGE to lignin results in reduction of hydrogen bonds via alkoxylation in the lignin molecule, which improves free volume, which is a free space in which the main molecules move inside the solution due to the repulsion of the neighboring molecules, in the molecule and thereby its mobility (Gordobil et al., 2017). The results for methylated kraft lignin also showed lower T_g (101 °C) values compared to kraft lignin, which was due to the reduction of hydroxy groups as some of them were converted to methoxy groups via methylation in the kraft lignin pretreatment. The T_g

values of methylated kraft lignin derivatives were found to be 69.46 °C, 68.53 °C, and 67.57 °C for MKL-1, MKL-2 and MKL-3, respectively.

Heat capacity at constant pressure (C_p) of the lignin samples were also listed in table 4.8. The C_p values show the amount of heat required to change the sample temperature by ΔT (Hatakeyama et al., 1982). The results showed that by increasing the ratio of DGE/lignin, the C_p values decreased as the introduction of aliphatic chain in the lignin molecule increases. The lignin macromolecules behave as collapsed rigid spheres in DMF solutions (when samples were prepared); however, via grafting a long aliphatic chain (DGE) into lignin, the interaction between lignin molecules decreases and thus the mobility of the chains increases. Therefore, the heat capacity decreases by increasing the free volume in kraft lignin molecule (Praharaj et al., 2015; Teng et al., 2013; Aslanzadeh et al. 2016). This behavior is attributed to enhancement in crosslinking and free volume of kraft lignin derivatives (Hatakeyama et al., 2009).

Table 4.8: Thermal properties of kraft lignin derivatives measured by DSC.

Lignins	**T_g (°C)**	**Heat capacity (J/g.°C)**
KL	154.33	0.2920
KL-1	116.82	0.2882
KL-2	89.23	0.2736
KL-3	70.19	0.2573
MKL	101.19	0.3386

MKL-1	69.46	0.2961
MKL-2	68.53	0.2741
MKL-3	67.57	0.2626

The T_g of lignin is affected by its molecular weight, crosslinking structure and hydrogen bonds (Heitner et al., 2010; Gordobil et al., 2017). As the amount of DGE was increased, its crosslinking and entanglement ability with aliphatic chain was enhanced, which caused a reduction in T_g values. As MKL had a higher molecular weight (Table 4.2), its C_p was higher. The above results suggest that crosslinked kraft lignin molecules (KL)s were not as dense as methylated kraft lignins, as the latter had higher C_p values (Hatakeyama et al., 2009). However, the production of kraft lignin derivatives via attaching long aliphatic chains proved that it is an appropriate method to obtain lignin based products with suitable glass transition temperatures (T_g) to use them in composites and polyols for polyurethane applications (Gordobil et al., 2017; Ahvazi et al., 2011).

4.6. Surfaces tension analysis

4.6.1. Contact angle of DMF solutions containing kraft lignin derivatives

The contact angle values of DMF solutions containing lignin derivatives are exhibited in Figure 4.10. The contact angle for DMF on glass slide was found to be <10 °, as reported previously (Janssen et al., 2006; Redón et al., 2006). From Figure 4.10, it is observed that 1) KL increased the contact angle of DMF on glass slide, 2) contact angle of the DMF increased with DGE content of KL, 3) DMF with MKL had a higher contact angle than KL and 4) increase in contact angle of DMF on glass slide with concentration of lignin samples. These results indicate that the

modification of lignin made it more solvophobic, and increased the surface tension of the DMF molecules. The addition of MKL increased contact angle of DMF more than KL, which shows that methylated kraft lignin was more solvophobic due to masking of phenolic hydroxy groups (Gordobil et al., 2017). Also, as the contact angle of modified lignin was higher than KL, these samples were more solvophobic than KL. This behavior is due to the reduction in the number of aromatic hydroxy groups by methylation. Further lignin modification with DGE incoporated liphophilc groups in lignin, and their solvophobicity increased and thus the interaction between DMF molecules increased resulting an increase in the contact angle values (Gordobil et al., 2017; Sen et al., 2015; Notley et al., 2010).

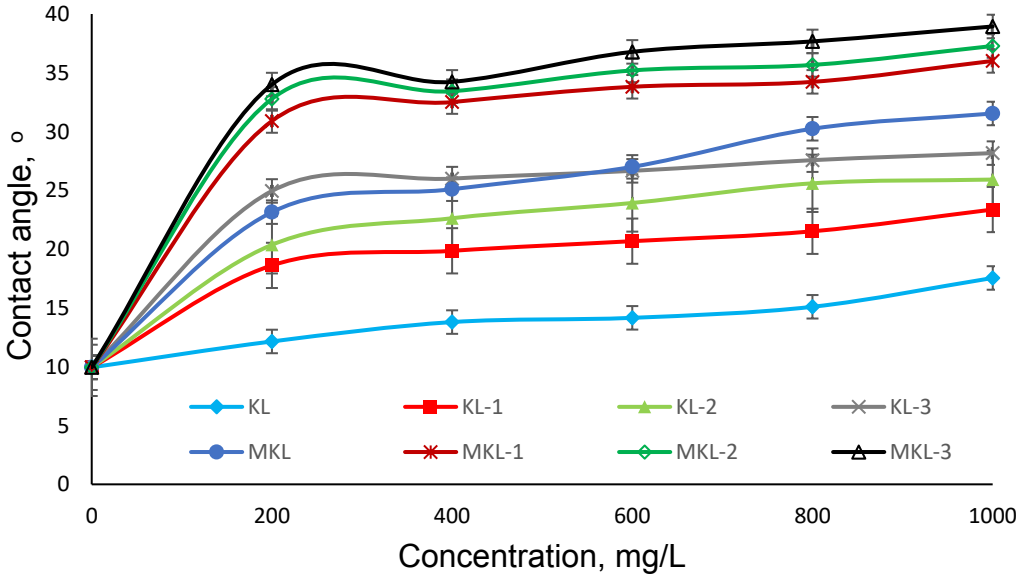

Figure 4.10: The effect of concentration of KLs and MKLs on the contact angle of DMF.

4.6.2. Surface tension of DMF solutions containing kraft lignin derivatives

The surface tension of DMF solutions containing KLs or MKLs (20 g/L) were investigated and the results were shown in Figure 4.11. In the absence of lignin samples, the surface tension of

DMF was found to be 27.9 mN/m. The addition of KL increased the surface tension of DMF to 31.66 mN/m, which is due to the fact that the interaction between the DMF molecules could increase by KL addition. Teng and others reported that the large macromolecules assemble in lignin/DMF solutions due to intra- and intermolecular π–π interactions between aromatic rings in lignin (Teng et al., 2013). In this phenomenon, the attractive forces between lignin molecules are stronger than the dispersive forces of DMF molecules and thus DMF surface tension increased by the addition of lignin (Praharaj et al., 2015; Aslanzadeh et al., 2016). The increase in DGE content of lignin samples further improved the surface tension of DMF with KL-1, KL-2 and KL-3 exhibiting surface tension values of 32.92, 35.02 and 37 mN/m, respectively. Furthermore, methylated kraft lignin samples also exhibited a similar trend. This behavior was probably due to the increased interaction between the DMF molecules as their solvophobicity was higher compared to KL.

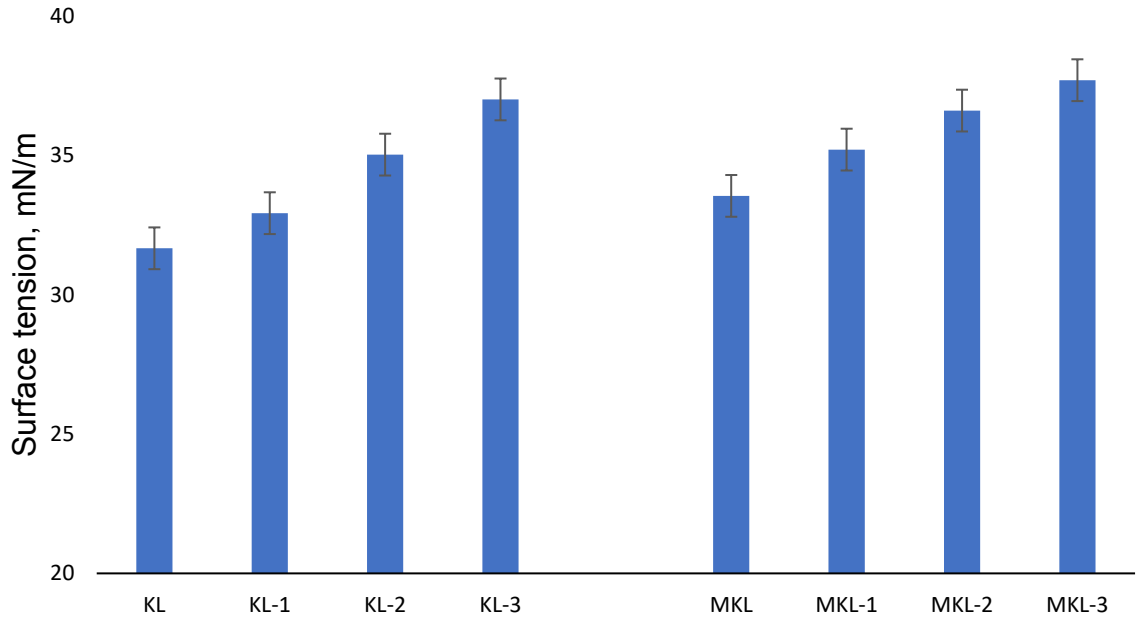

Figure 4.11: Surface tension of DMF solutions containing KLs and MKLs at a concentration of 20 g/L and temperature (22 °C).

To investigate the effect of concentration of lignin derivatives on the surface tension of DMF, the surface tension of DMF was measured at varying concentrations (200 -1000 mg/L) of unmodified or modified lignin samples at room temperature and the results were shown in Figure 4.12. By increasing the concentrations of lignin derivatives, the surface tension of DMF was improved implying that at a concentration of 1000 mg/L, MKL-3 caused the maximum upsurge in the surface tension of DMF (36.29 mN/m).

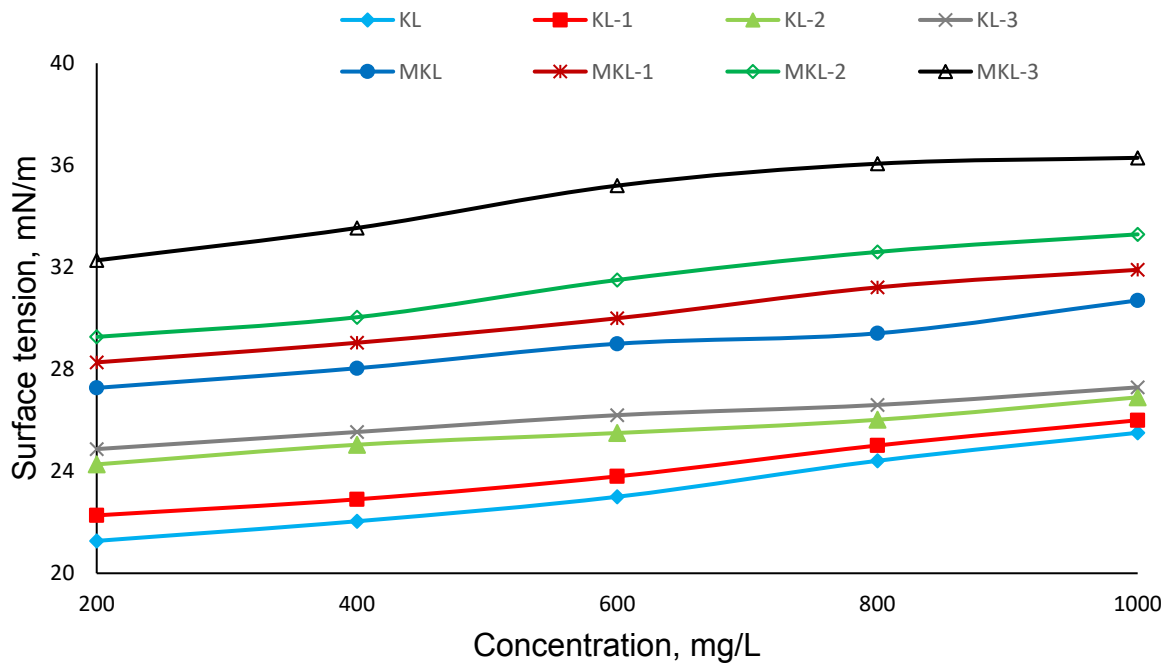

Figure 4.12: Surface tension of DMF at various concentrations (200-1000 mg/L) of KLs or MKLs and room temperature.

4.6.3. Interfacial tension of DMF solutions containing kraft lignin derivatives

Figure 4.13 exhibits the effect of lignin derivatives on interfacial tension between DMF and glass slide.

The interfacial tension between DMF and glass slide was increased due to addition of kraft lignin derivatives as γ_{SV} for glass slide was 12.3 mN/m. The addition of KL increased the interfacial tension between DMF and glass slide and this was further increased with using grafted KLs. This is in good agreement with surface tension results in Figure 4.12. MKL-3 caused the maximum increase in the interfacial tension (18 mN/m), which is possibly due to its maximum DGE grafting ratio. A similar behavior was observed for MKLs.

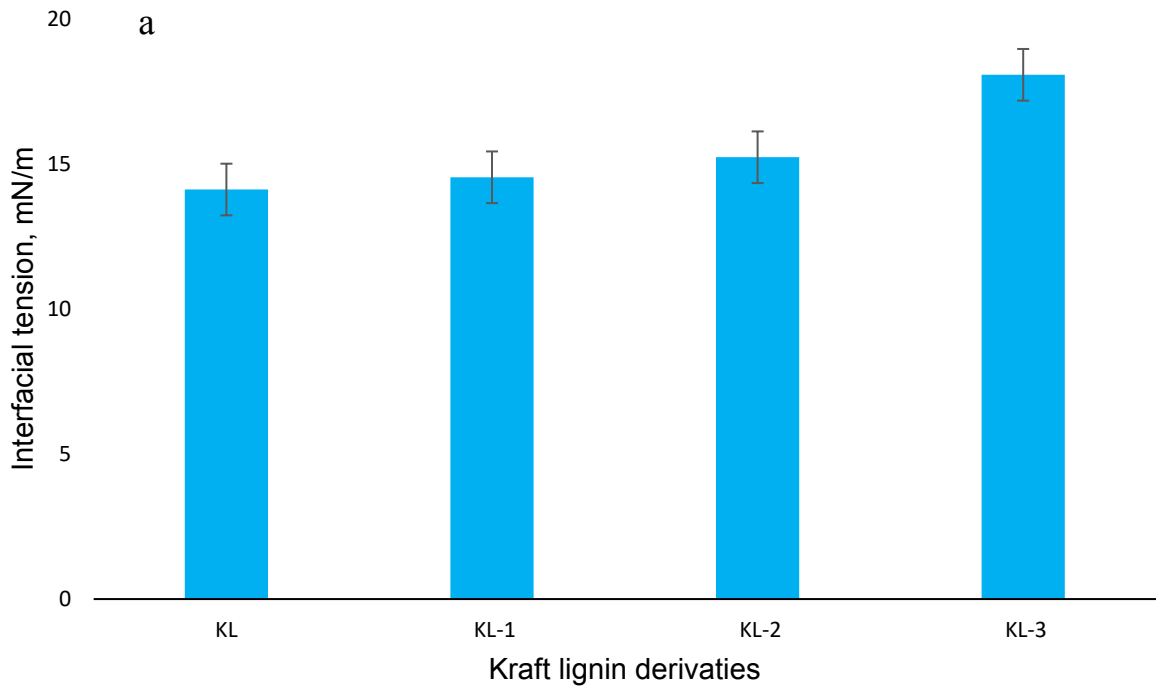

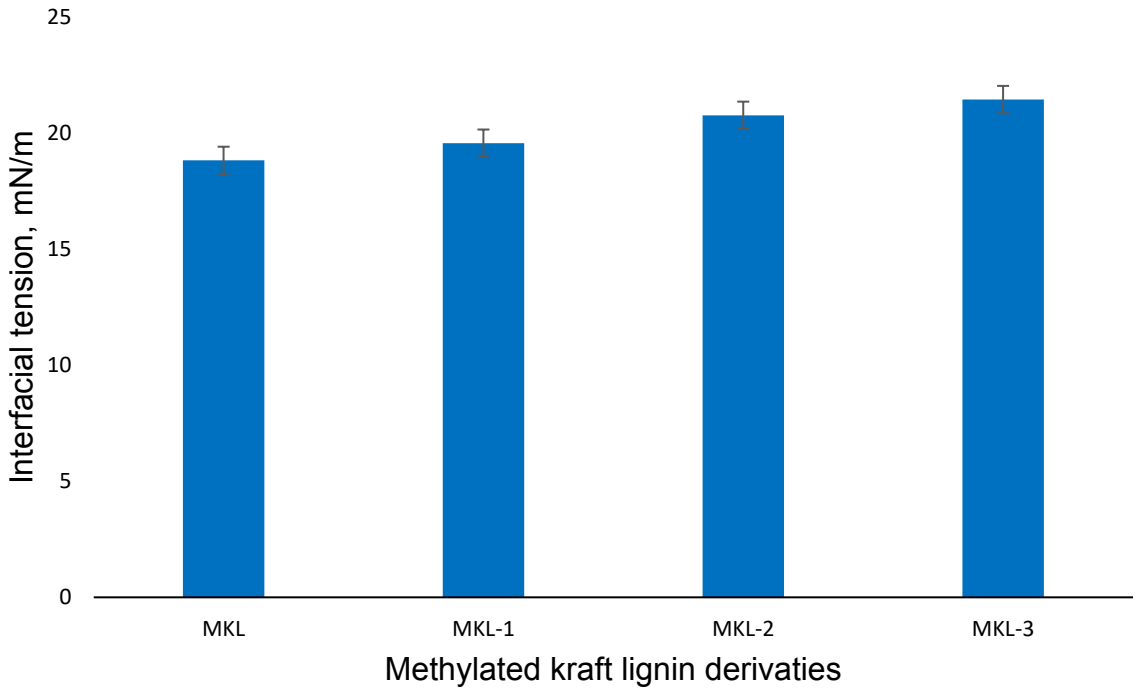

Figure 4.13: Effect of a) KL derivatives and b) MKL derivatives interfacial tension between DMF and glass slide.

4.6.4. Contact angle of water droplet on glass slide coated with kraft lignin derivatives

The contact angle that water droplet made with the surface of a glass slide coated with kraft lignin derivatives were analyzed as a function of time, spinning rate, solvents, and drying temperature. The initial equilibrium contact angle of water was 21° on uncoated glass slide (Redón et al., 2006; Janssen et al., 2006). However, contact angle of water did decrease over time to various levels in 2 min of experiments. The results obtained under different conditions imply if the film was relatively non-swelling and non-porous.

4.6.4.1. The effect of solvent type on the contact angle of coated film

The solvent type reported to greatly influence the contact angle of the surface it made (Janssen et al., 2006; Norgren et al., 2006). Figure 4.14 displays the contact angle of water drop with the lignin

derivative films that were formed using different solvents. It is observed that 1) the contact angle was significantly affected by the type of solvent used, 2) by increasing the DGE grafting ratio, the hydrophobicity of the surfaces increased, 3) more noticeable change was observed for the samples prepared with ammonium hydroxide as solvent and 4) the contact angle of methylated samples was higher. The reason for more noticeable change in hydrophobicity of the surface for the samples prepared in ammonium hydroxide could be related to the surface texture of films.

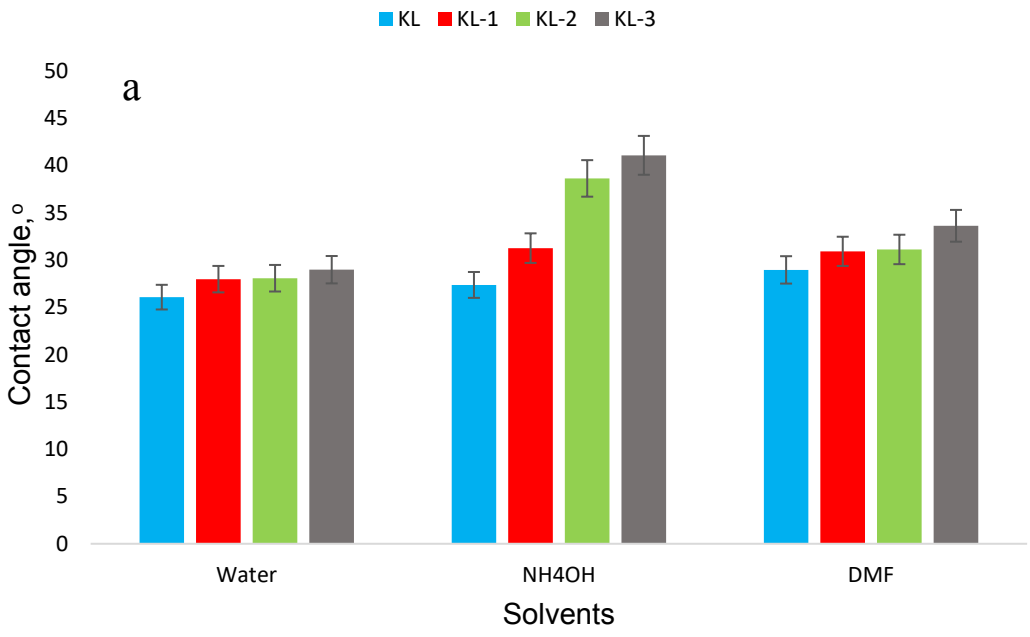

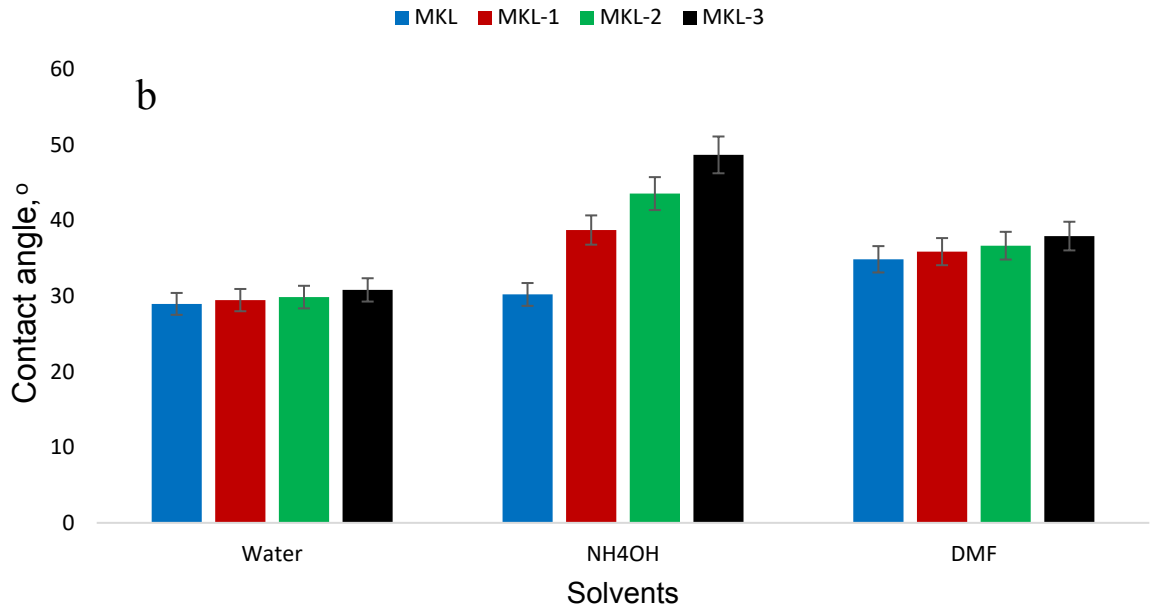

Figure 4.14: The effect of solvent on the contact angle of the surface coated with a) kraft lignin derivatives and b) methylated kraft lignin derivatives, recorded at 20 s and 22 ℃.

Figure 4.15 presents the SEM images of glass slides coated with different solutions containing lignin derivatives. The surface treated with water showed the non-uniform surface, while dimethylformamide formed smooth surface. However, the surface treated with ammonium hydroxide solution had more roughness. It was reported in the literature that an increase in surface roughness could improve its hydrophobicity (Norgren et al., 2006).

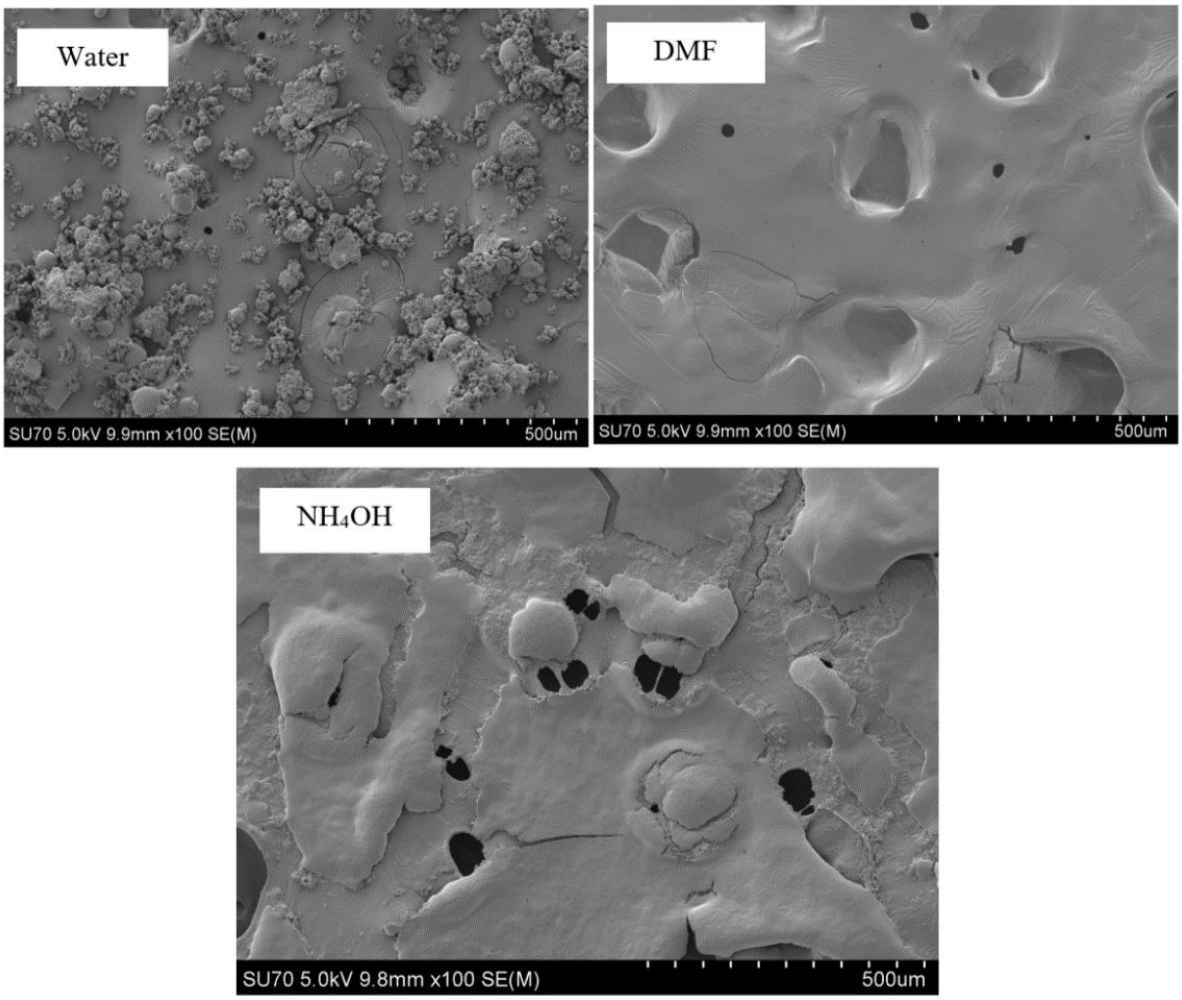

Figure 4.15: SEM images of glass slides coated with different solutions containing KL-3, 10 g/L.

Furthermore, as methylation covers the phenolic –OH of kraft lignin, it makes it more hydrophobic and thus its further modification with DGE enhances the hydrophobicity of the surface to a greater extent (Sen et al., 2015; Gordobil et al., 2017; Notley et al., 2010).

4.6.4.2. The effect of spinning rate on the contact angle of coated film

As reported previously (Norgren et al., 2006), the contact angle decreased by lowering the film thickness via increasing rotation speed of film making (rpm). The contact angle of the surfaces coated with kraft lignin derivatives is shown in Figure 4.16 as a function of coating spinning rates.

It is observed that by enhancing the speed from 500 to 1000 rpm, the contact angle generally dropped implying an increase in the hydrophilicity of the surface, and the reason for this behavior may be ascribed to a thinner layer of coating layers that can be made at higher rotational speed (Norgren et al., 2006).

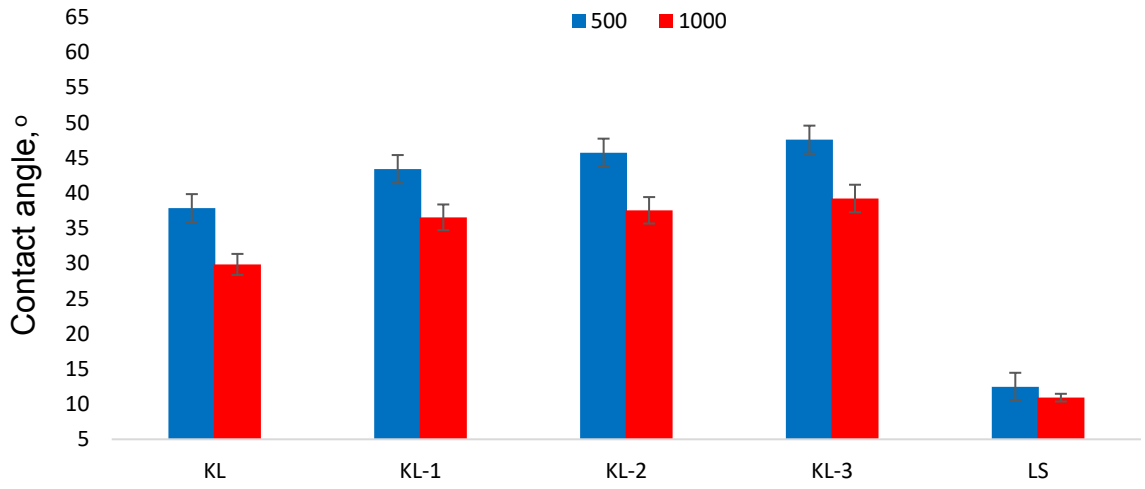

Figure 4.16: Contact angle of water droplet on a surface coated with kraft lignin derivatives at different spinning rates.

4.6.7. The effect of temperature of coating process on contact angle

Figure 4.17 shows the impact of coating temperature on the hydrophobicity of the coated film for water droplet. It is seen that the contact angle of water on coated films was higher at lower coating temperature. The reason for this behavior may be attributed to a better coating performance of the surface at lower temperature, as higher temperature may generate bubbles and harsher evaporation conditions that would affect the surface of coated film (Hu et al., 2002; Norgren et al., 2006; Erbil, H., 2006).

It is also seen that the temperature affected the contact angle of the surfaces containing unmodified samples more greatly than methylated samples. The reason for this behavior is due to the existence

of hydrogen bond in unmodified kraft lignin which cause nonuniformity and instability in the surfaces due to the fast solvent evaporation. In other words, methylated kraft lignin derivatives were less affected by temperature due to the phenolic hydroxy groups masking in the pretreatment step (Griffini et al., 2015).

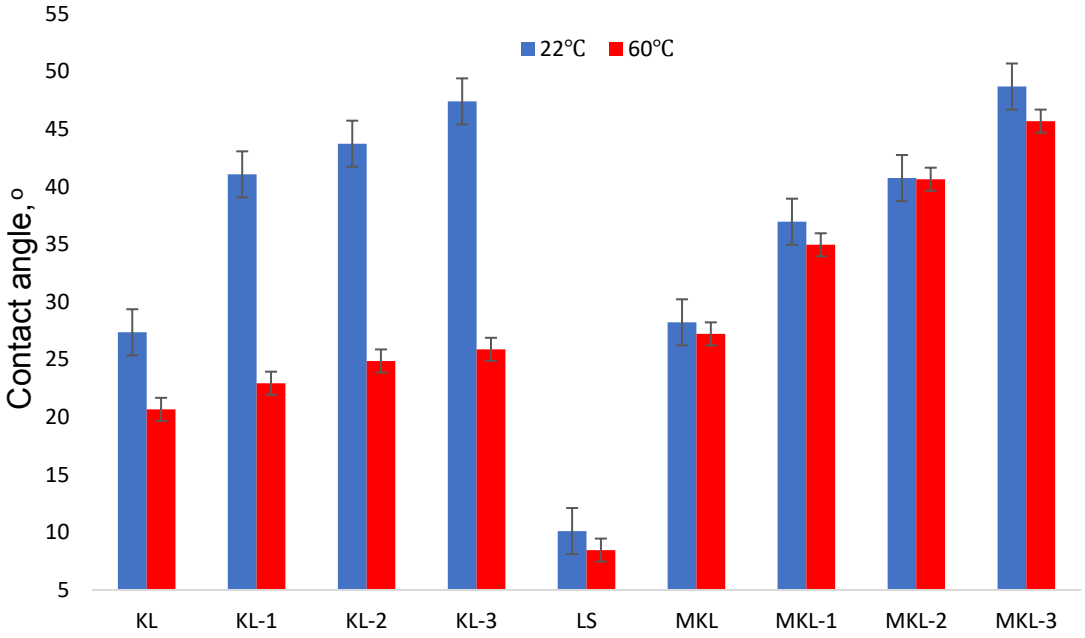

Figure 4.17: The effect of temperature of film formation on the contact angle of water droplet and coated glass slide (lignin derivatives in NH_4OH solution coated at 500 rpm).

4.6.4.3. The effect of time on the contact angle of water droplet

The contact angle of water droplet on the surface of the glass slide coated with various lignin samples is shown in figure 4.18. Three samples of KL, KL-3 and lignosulfonate (LS) were chosen in this test due to significant variations in the hydrophobicity of their films. Among the three samples, the contact angle between water droplet and the film coated with KL-3 was higher at both 5 s (50 °) and 20 s (39 °), while the contact angle between water droplet and film coated with LS substrate was lower. This indicates that KL-3 made the most hydrophobic surface and LS made

the most hydrophilic surface. It is also clear that the contact angle did decrease over time in all substrates. However, even though the reduction rate was different between the surfaces, the contact angle showed the same trend at both time intervals recorded (5 s and 20 s). Furthermore, by extending the time of contact, the contact angle of the water droplet on all surfaces was reduced. This could be due to the water evaporation or some minor swelling of the film (Norgren et al., 2006).

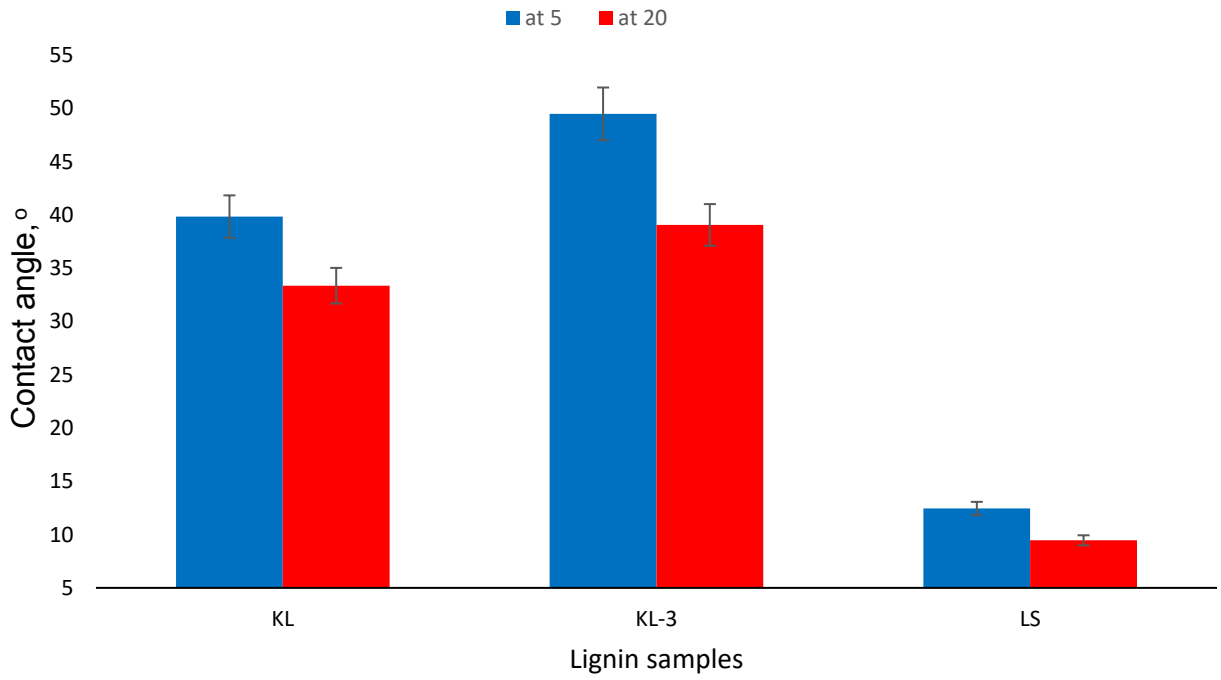

Figure 4.18: Contact angle of water droplet on glass slide coated with KL, KL-3 and LS dissolved in ammonium hydroxide solution after 5 s and 20 s of time intervals.

References

Ahvazi, B., Wojciechowicz, O., Ton-That, T., Hawari, J. 2011. Preparation of Lignopolyols from Wheat Straw Soda Lignin. Journal of Agricultural and Food Chemistry, 59(19), 10505-10516.

Alkhalifa, Z. 2017. Copolymerization of pretreated kraft lignin and acrylic acid to produce flocculants for suspension and solution systems. Lakehead University. Mater thesis.

Argyropoulos, D., Sadeghifar, H., Cui, C., Sen, S. 2014. Synthesis and characterization of poly(arylene ether sulfone) kraft lignin heat stable copolymers. ACS Sustainable Chemistry and Engineering. 2(2), 264-271.

Aslanzadeh, S., Zhu, Z., Luo, Q., Ahvazi, B., Boluk, Y., Ayranci, C. 2016. Electrospinning of colloidal lignin in poly(ethylene oxide)N,N-dimethylformamide solutions. Macromolecular Materials and Engineering, 301(4), 401-413.

Bertram, J. L. 1972. Glycidyl ethers of haloneopentyl glycols. U.S. Patent. 3,686,358.

Brebu, M., Vasile, C. 2010. Thermal degradation of lignin- A review. Cellulose Chemistry Technology. 44(9), 353-363.

Chen, C., Li, M., Wu, Y., Sun, R. 2014. Modification of lignin with dodecyl glycidyl ether and chlorosulfonic acid for preparation of anionic surfactant. RSC Advances, 4(33), 16944-16950.

Duraibabu, D., Alagar, M., Kumar, S. 2014. Studies on mechanical, thermal and dynamic mechanical properties of functionalized nanoalumina reinforced sulphone ether linked tetraglycidyl epoxy nanocomposites. RSC Advance. 4(76), 40132-40140.

Erbil, H. 2006. Surface chemistry of solid and liquid interfaces. Oxford: Blackwell Pub.

Gan L, Zhou M, Yang D, Qiu X. 2013. Preparation and evaluation of carboxymethylated lignin as a dispersant for aqueous graphite suspension using Turbiscan Lab Analyzer. Journal of Dispersion Science and Technology. 34, 644-650.

Garcia, F. Soares, B. 2003. Determination of the epoxide equivalent weight of epoxy resins based on diglycidyl ether of bisphenol A (DGEBA) by proton nuclear magnetic resonance. Polymer Testing. 22(1), 51-56.

Garea, S., Corbu, A., Deleanu, C., Iovu, H. 2006. Determination of the epoxide equivalent weight (EEW) of epoxy resins with different chemical structure and functionality using GPC and 1H-NMR. Polymer Testing. 25(1), 107-113.

Gordobil, O., Herrera, R., Llano-Ponte, R., Labidi, J. 2017. Esterified organosolv lignin as hydrophobic agent for use on wood products. Progress In Organic Coatings. 103, 143-151.

Griffini, G., Passoni, V., Suriano, R., Levi, M., Turri, S. 2015. Polyurethane coatings based on chemically unmodified fractionated lignin. ACS Sustainable Chemistry and Engineering. 3(6), 1145-1154.

Hatakeyama, H., Hatakeyama, T. 2009. Lignin structure, properties, and applications. Biopolymers. 1-63.

Hatakeyama, T., Nakamura, K., Hatakeyama, H. 1982. Studies on heat capacity of cellulose and lignin by differential scanning calorimetry. Polymer. 23(12), 1801-1804.

Heitner, C., Dimmel, D., Schmidt, J. 2010. Lignin and lignans: Advances in chemistry. Boca Raton, FL: CRC Press, Taylor and Francis. ISBN: 978-1-4200-1580-5.

Hou, S., Chung, Y., Chan, C., Kuo, P. 2000. Function and performance of silicone copolymer. Part IV. Curing behavior and characterization of epoxy–siloxane copolymers blended with diglycidyl ether of bisphenol-A. Polymer. 41(9), 3263-3272.

Hu, T. 2002. Chemical modification, properties, and usage of Lignin. New York: Springer. ISBN: 978-1-4615-0643-0

Janssen, D., De Palma, R., Verlaak, S., Heremans, P., Dehaen, W. 2006. Static solvent contact angle measurements, surface free energy and wettability determination of various self-assembled monolayers on silicon dioxide. Thin Solid Films. 515(4), 1433-1438.

Konduri, M. 2017. New generation of dispersants by grafting lignin or xylan. Lakehead university. Doctoral dissertation.

Labbé, A., Brocas, A., Ibarboure, E., Ishizone, T., Hirao, A., Deffieux, A., Carlotti, S. 2011. Selective ring-opening polymerization of glycidyl methacrylate: Toward the synthesis of cross-linked (co)polyethers with thermoresponsive properties. Macromolecules. 44(16), 6356-6364.

Laurichesse, S., Huillet, C., Avérous, L. 2014. Original polyols based on organosolv lignin and fatty acids: new bio-based building blocks for segmented polyurethane synthesis. Green Chemistry. 16(8), 3958-3970.

Norgren, M., Notley, S., Majtnerova, A., Gellerstedt, G. 2006. Smooth model surfaces from lignin derivatives. I. Preparation and characterization. Langmuir. 22(3), 1209-1214.

Notley, S., Norgren, M. 2010. Surface energy and wettability of spin-coated thin films of lignin isolated from wood. Langmuir. 26(8), 5484-5490.

Passoni, V., Scarica, C., Levi, M., Turri, S., Griffini, G. 2016. Fractionation of industrial softwood kraft lignin: Solvent selection as a tool for tailored material properties. ACS Sustainable Chemistry and Engineering., 4(4), 2232-2242.

Praharaj, M., Mishra, S., 2015. Comparative study of molecular interaction in ternary liquid mixtures of polar and non-polar solvents. Journal of Pure and Applied Ultrasonics. 37, 68-77.

Redón, R., Vázquez-Olmos, A., Mata-Zamora, M., Ordóñez-Medrano, A., Rivera-Torres, F., Saniger, J. 2006. Contact angle studies on anodic porous alumina. Journal Of Colloid And Interface Science. 287(2), 664-670.

Renner, A., Grütter, P., Hügi, R. 1985. Novel tetraglycidyl ethers. U.S. Patent. 4,549,008

Rowell, R. Chen, G. 1994. Epichlorohydrin coupling reactions with wood. Wood Science and Technology. 28(5), 371-376.

Sadeghifar, H., Cui, C., Argyropoulos, D. 2012. Toward thermoplastic lignin polymers. Part 1. Selective masking of phenolic hydroxyl groups in kraft lignins via methylation and oxypropylation chemistries. Industrial and Engineering Chemistry Research. 51(51), 16713-16720.

Samuel, R., Pu, Y., Jiang, N., Fu, C., Wang, Z., Ragauskas, A. 2014. Structural characterization of lignin in wild-type versus COMT Down-Regulated Switchgrass. Frontiers in Energy Research, 1, 1-9.

Sen, S., Patil, S., Argyropoulos, D. 2015. Methylation of softwood kraft lignin with dimethyl carbonate. Green Chemistry. 17(2), 1077-1087.

Sen, S., Sadeghifar, H., Argyropoulos, D. 2013. Kraft lignin chain extension chemistry via propargylation, oxidative coupling, and claisen rearrangement. Biomacromolecules. 14(10), 3399-3408.

Tänzer, W., Reinhardt, S., Fedtke, M. 1993. Reaction of glycidyl ethers with aliphatic alcohols in the presence of benzyl dimethylamine. Polymer. 34(16), 3520-3525.

Teng, N., Dallmeyer, I., Kadla, J. 2013. Effect of softwood kraft lignin fractionation on the dispersion of multiwalled carbon nanotubes. Industrial and Engineering Chemistry Research. 52(19), 6311-6317.

Wu, H., Chen, F., Feng, Q., Yue, X. 2012. Oxidation and sulfomethylation of alkali-extracted lignin from corn stalk. BioResources. 7(3), 2742-2751.

Zech, J. 1951. Epoxide preparation. U.S. Patent. 2,538,072.

Zhang, J., Feng, L., Wang, D., Zhang, R., Liu, G., Cheng, G. 2014. Thermogravimetric analysis of lignocellulosic biomass with ionic liquid pretreatment. Bioresource Technology. 153, 379-382.

Chapter 5: Conclusions and recommendations for future work

5.1. Overall conclusions

The present work successfully demonstrated grafting of long chain dodecyl glycidyl ether (DGE) to kraft lignin in the presence of N,N-dimethylbenzylamine as a catalyst. The impact of methylation to mask the phenolic hydroxide of lignin was also investigated. The results showed that the glycidyl ether chain was grafted to carboxylate groups when DGE/lignin ratio was low. At a higher ratio, the phenolic hydroxy would also react with DGE.

Kraft lignin was successfully pretreated with dimethyl sulfate to mask the phenolic hydroxy groups at 80 °C. ^{31}P NMR and titration confirmed the conversion of hydroxy groups to methoxy groups as the total phenolic–OH groups (Condensed and non-condensed) were significantly decreased from 1.15 to 0.14 mmol/g, and from 1.20 to 0.12 mmol/g, respectively. Moreover, the aliphatic hydroxy groups were unaffected by kraft lignin pretreatment as confirmed by titration.

^{31}P NMR also confirmed the grafting ratio of DGE on unmodified and modified kraft lignin. Interestingly, DGE was grafted at the carboxylate group first due to its higher acidity. By increasing the DGE/lignin ratio, the phenolic–OH decreased. This observation indicates that DGE was successfully grafted to lignin. The results on the methylated kraft lignin were similar to untreated kraft lignin, but lower grafting ratios were obtained as the phenolic–OH groups were masked in the pretreatment step.

The thermal behavior of lignin derivatives was studied by TGA and DSC. Generally, grafting DGE to kraft lignin reduced its thermal stability as well as glass transition temperature. However, modified kraft lignin derivates showed worse thermal stability than unmodified ones which was

due to the reduction of hydrogen bonds between the molecules by methylation and increase in crosslinking and entanglement of molecules via alkoxylation.

Furthermore, by increasing the grafting ratio of DGE/lignin, the hydrophobicity of lignin based products was enhanced, and the surface tension, contact angle and interfacial tension of DMF increased by methylation. The surface tension and contact angle of DMF as well as the intenrfacial tension between glass slide and DMF were 27.9 mN/m, 9.95 ° and 13.93 mN/m, respectively. The surface tension and contact angle of DMF as well as the interfacial tension between the glass slide and DMF were increased to 30.7 mN/m, 31.54 °, and 18.83 mN/m, respectively when 1000 mg/L of MKL was dissolved in DMF. The surface tenstion and contact angle of DMF as well as the interfacial tenstion of glass slide and DMF were increased to 36.29 mN/m, 38.94 °, and 21.45 mN/m when 1000 mg/L of MKL-3 was dissolved in DMF. Moreover, the contact angle of water droplet was 21° on a glass slide, but it was increased to 41.06 °, 48.68 °, respectively, for glass slides coated with KL-3 and MKL-3. The solvent used for coating glass slides, the spinning rate and and the temperature of drying had significant impacts on the surface roughness and thus hydrophobicity of coated glass slides.

5.2. Recommendations for future work

In this study, the results suggested that kraft lignin derivatives with high hydrophobicity could be obtained. In future, the hydrophobic modification of lignin could also be conducted with a chemical that has a higher alkyl chain. The application of the products on composites would disclose the potential use of these lignin based products. The sulfonation of the lignin derivatives might also show potential to produce sulfonated products for different applications, and thus recommended as future work.